


 Cite this: *Green Chem.*, 2024, **26**, 8123

# Emerging applications of deep eutectic solvents in the preparation and functionalization of biomass-derived carbonaceous materials: challenges and prospects†

 Yiyi Shen,<sup>‡a,b</sup> Haiqin Zhou,<sup>‡a,b</sup> Xiaotong He,<sup>a,b</sup> Feng Shen,<sup>id c</sup> Zhixiang Xu,<sup>id d</sup> Bo Yang,<sup>e</sup> Lingzhao Kong<sup>id f</sup> and Lichun Dai<sup>id \*a,b</sup>

Biomass-derived carbonaceous materials (BCMs) have been extensively applied in diverse areas, attributed to their recognized sustainability, low cost, diverse and scalable synthesis routes, and tunable structure and function. Recently, deep eutectic solvents (DESs), a class of novel and green solvents, have emerged as a promising alternative to traditional solvents and processing techniques for the preparation and functionalization of BCMs for various applications. However, there is still a knowledge gap regarding the applications of DESs in the preparation and functionalization of BCMs. Considering these, this review summarizes the emerging applications of DESs in the preparation and functionalization of BCMs, including their use as biomass pretreatment solvents, carbon precursors, soft templates, solvothermal carbonization (STC) media, and post-modification agents. This review also discusses the applications of the resultant BCMs in various fields, such as pollution control, energy storage, and biocatalysis, and highlights the challenges and prospects for using DESs in the preparation and functionalization of BCMs. Overall, the use of designer DESs in the preparation and functionalization of BCMs has the potential to contribute to the development of sustainable and cost-effective technologies for a wide range of applications.

 Received 1st April 2024,  
Accepted 4th June 2024  
DOI: 10.1039/d4gc01579g  
rsc.li/greenchem

## 1. Introduction

Carbon materials, such as classic coal,<sup>1</sup> graphite<sup>2</sup> and activated carbon (AC),<sup>3</sup> and novel fullerenes,<sup>4</sup> carbon nanotubes,<sup>5</sup> graphene<sup>6</sup> and graphdiyne,<sup>7</sup> have been extensively explored in recent decades for their applications in various important fields. However, most of them are prepared from non-renewable sources *via* energy- and/or chemical-intensive conditions.<sup>8,9</sup> It is imperative to develop carbon materials

using low-cost and sustainable carbon sources under environmentally friendly conditions. Owing to these concerns, BCMs, as biomass-derived carbon materials, have received considerable attention ascribed to their sustainable and abundant biomass sources, diverse preparation routes, tunable structures and properties, and versatile applications.<sup>10–14</sup>

A variety of techniques can be employed to synthesize BCMs *via* pyrolysis,<sup>15,16</sup> hydrothermal carbonization (HTC),<sup>17,18</sup> ionothermal carbonization (ITC)<sup>19–21</sup> and other carbonization routes, and to functionalize BCMs *via* heteroatom doping, activation, oxidation, recombination and others. Recently, deep eutectic solvents (DESs), a class of novel and green solvents, have emerged as a promising alternative to traditional solvents and processing techniques for the synthesis and/or functionalization of BCMs for applications in various fields (Table S1†).<sup>12,22,23</sup> For example, we applied a Type III DES composed of choline chloride (ChCl) and citric acid (CA) as a reusable carbonization medium for the synthesis of a BCM with co-enriched carboxyl and phenol groups toward high efficiency adsorption and reduction of uranium,<sup>23</sup> and Aruchamy *et al.* prepared functional carbon helices as an enzyme host by carbonizing *Parthenium hysterophorus* in a Type I DES composed of ChCl and FeCl<sub>3</sub> at 150–250 °C for 6–24 h.<sup>24</sup> Besides the application of DESs as the carbonization medium, they also

<sup>a</sup>Key Laboratory of Development and Application of Rural Renewable Energy, Biogas Institute of Ministry of Agriculture and Rural Affairs, Chengdu 610041, Sichuan, China. E-mail: daulichun@caas.cn

<sup>b</sup>Research Center for Rural Energy and Ecology, Chinese Academy of Agricultural Sciences, Chengdu 610041, Sichuan, China

<sup>c</sup>Agro-Environmental Protection Institute, Chinese Academy of Agricultural Sciences, No. 31, Fukang Road, Nankai District, Tianjin 300191, China

<sup>d</sup>School of Energy and Power Engineering, Jiangsu University, Zhenjiang 212013, China

<sup>e</sup>Zhai Mingguo Academician Work Station, Sanya University, Sanya 572022, China

<sup>f</sup>School of Environmental Science and Engineering, Suzhou University of Science and Technology, Suzhou 215009, China

†Electronic supplementary information (ESI) available. See DOI: <https://doi.org/10.1039/d4gc01579g>

‡These two authors contributed equally to this work.



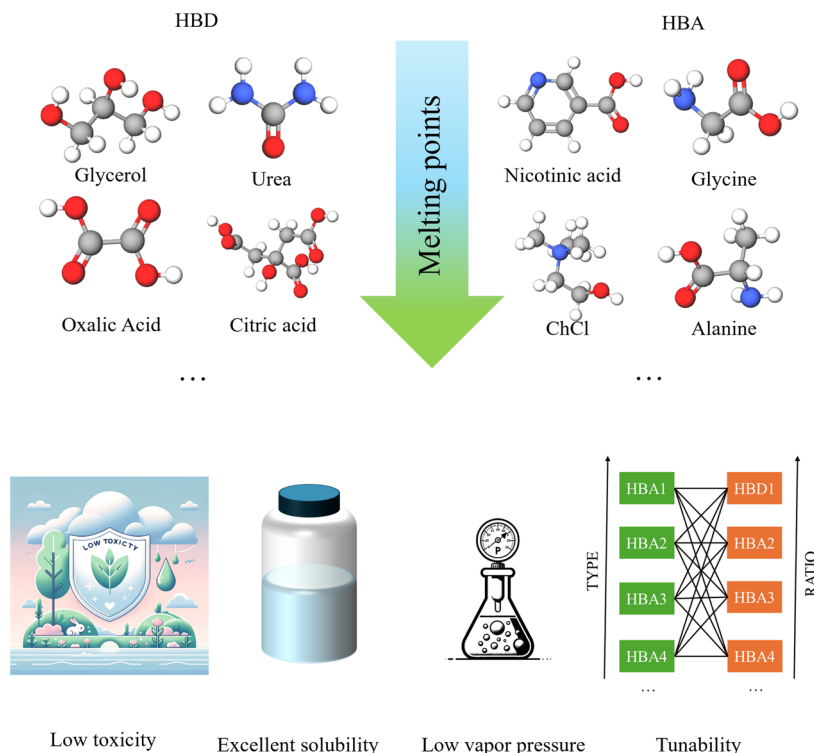


Fig. 1 Composition and unique properties of DESs.

can be applied as the carbon source using DESs composed of biomass derivatives,<sup>25,26</sup> as biomass pretreatment solvents before the synthesis of BCM,<sup>27–29</sup> or as impregnation agents for BCM surface modification.<sup>30–32</sup> However, although DESs have shown their immense potential in the synthesis and functionalization of BCMs, little comprehensive knowledge and perspectives are available on the preparation and functionalization of BCMs mediated by DESs.

DESs are composed of a hydrogen bond donor (HBD) and an acceptor, characterized by remarkable declines in melting points compared to those of the components, and known for their low toxicity, low vapor pressure and excellent solubility for a wide range of organic and inorganic compounds (Fig. 1).<sup>33–35</sup> They are a class of green solvents to replace ionic liquids (ILs), while ILs tend to be more expensive than DESs, are often nonbiodegradable and highly toxic. They are promising as inexpensive designer solvents with tunable components and physicochemical properties. There are five types of DESs, based on the types of HBDs and hydrogen bond acceptors (HBAs) used for the preparation of DESs.<sup>33</sup> To keep up the pace of rapid progress in the emerging applications of DESs in the preparation and functionalization of BCMs, a timely overview is needed to provide perspective on the synthesis and functionalization of BCMs mediated by DESs and to push back the boundaries of knowledge for both DESs and BCMs. This review describes the status of the use of DESs in the preparation and functionalization of BCMs along with highlighting the applications of the resultant BCMs in various fields.

Finally, this review also analyzes the future challenges and research directions in this field.

## 2. DESs for functional BCM preparation

### 2.1 DESs as processing solvents before biomass carbonization

**2.1.1 DESs as biomass pretreatment solvents.** Biomass pretreatment can adjust the physicochemical structure of the feedstock, which plays an important role in the synthesis of BCMs.<sup>36,37</sup> Various solutions under various conditions have been used for the pretreatment of biomass, *e.g.*, hydrothermal pretreatment<sup>38,39</sup> and solvothermal pretreatment with ethanol for the preparation of porous carbon from bagasse.<sup>40</sup> DESs have been extensively used for the pretreatment or fractionation of biomass.<sup>41–44</sup> Recently, DESs have been further employed as solvents to pretreat biomass for BCM preparation (Table 1), *e.g.*, pretreatment of palm fiber with a DES composed of ChCl and urea for AC preparation,<sup>37</sup> pretreatment of kraft lignin with a DES composed of ChCl and formic acid for the preparation of ordered mesoporous carbon,<sup>36</sup> pretreatment of wheat straw with a DES composed of ChCl and LA at 90 °C for 12 h for the cascaded preparation of carbon dots (CDs) from DES-extractable lignin and Mg-Fe oxide-doped BCM from DES-insoluble wheat straw fractions,<sup>45</sup> pretreatment of poplar wood powder with a DES composed of ChCl and LA at



**Table 1** Pretreatment of biomass with DES for functional BCM preparation

Biomass	DES components (molar ratio)	Pretreatment conditions	Carbonization conditions of pretreated biomass	Application of the resultant carbon	Ref.
1 Palm fibre	ChCl : urea = 1 : 2	1 : 5 solid to liquid ratio, 4 h, 110 °C	Activation at 900 °C, 1 h, 1 L min <sup>-1</sup> CO <sub>2</sub>	Adsorption (Pb)	37
2 Pine residues	ChCl : urea = 1 : 2 MPTB : EG = 1 : 4	1 : 10 biomass to DES, 25 °C, 300 rpm, 1 h	HTC at 180–260 °C for 30 min at 150 rpm		47
3 Lignin	Urea : ChCl : gly = 1 : 1 : 1	18% lignin, 80 °C, 2 h	Etherification with PEGDE at 90 °C for 24 h, followed by successive solvent displacement with ethanol and water, freeze-drying, and carbonization in CO <sub>2</sub> at 750 °C for 5 h	3 D hierarchical porous carbon for supercapacitors	48
4 Lignin	ChCl : formic acid (1 : 1–4)	1 : 20 mass ratio, 90–150 °C, 1–7.5 h	Pretreated lignin in alkaline ethanol solution was mixed with formaldehyde to form resin, and then thermal polymerization and carbonization were conducted	Ordered mesoporous carbon for supercapacitors	36
5 Rice husk	ChCl : OA = 1 : 2 ChCl : EG = 1 : 1 ChCl : urea = 1 : 1	100 °C for 4 h	Mixed with magnesium at a 1 : 1 weight ratio, and cryogenic milling method for 1 min at 30 Hz, carbonization in N <sub>2</sub> at 850 °C for 2 h	Anode materials for lithium-ion batteries	29
6 Sewage sludge	Boric acid : urea : water 4.82 : 3.6 : 100 (mass ratio)	100 °C for 2 h	700, 800, or 900 °C for 1 h, 20 °C min <sup>-1</sup> N <sub>2</sub>	Electrochemical applications	46
7 Wheat straw	ChCl : LA = 1 : 15	1 : 10 mass ratio, 90 °C, 12h	LCDs: 180 °C for 6 h, 10 000 rpm for 10 min, dialyzed with a 2000 kDa, freeze-dried Mix 100 mL water and 5 g at 200 rpm, for 30 min, drop MgCl <sub>2</sub> ·6H <sub>2</sub> O : FeCl <sub>3</sub> ·6H <sub>2</sub> O (1 : 2) and adjust pH to 10, 800 °C for 1 h, 5 °C min <sup>-1</sup> N <sub>2</sub>	Fluorescence sensing Activate PDS for arbidol degradation	45
8 Poplar wood	ChCl : LA = 1 : 9	1 g : 50 ml DES, 120 °C, 6 h	800 °C, 5 °C min <sup>-1</sup> N <sub>2</sub> , 2 h	Electrode for supercapacitors	27

120 °C for 6 h to extract lignin for the preparation of porous carbon from lignin,<sup>27</sup> pretreatment of rice husk for the preparation of silicon/carbon composites,<sup>29</sup> and pretreatment of sewage sludge with a DES composed of boric acid and urea for the preparation of B,N co-doped carbon.<sup>46</sup> Specifically, Chia and Yoon employed a Type III DES composed of ChCl and urea (1 : 2 molar ratio) to pretreat palm fiber at a solid to liquid ratio of 1 : 5 before the carbonization and activation process.<sup>37</sup> The resultant AC pretreated with the DES was more efficient than the ACs obtained from the pre-impregnation with H<sub>2</sub>SO<sub>4</sub> or NaOH in Pb and NO<sub>3</sub>-N adsorptive removal.<sup>37</sup>

It has been reported that Type III DESs promote the cleavage of unstable ether bonds in the phenylpropane units of lignin and the deconstruction of C–C bonds, resulting in the reduction of lignin molecular weight and the increase of phenolic hydroxyl content.<sup>49,50</sup> Thus, Sima *et al.* employed a Type III DES composed of ChCl and formic acid to pretreat the masson pine alkali lignin.<sup>36</sup> Owing to the increase of phenolic groups and the decrease of molecular weight of lignin, the DES-pretreated lignin was more reactive toward formaldehyde to form resin, favoring the formation of ordered mesoporous carbon.<sup>36</sup> Consequently, the resultant carbon material showed a much higher BET surface area and a much greater specific capacitance.<sup>36</sup>

Based on these results, we can find that the pretreatment of biomass with DESs favors the preparation of porous and/or monolithic BCMS. However, there is a lack of comparison between the treatments with emerging DESs and conventional solutions. Some of the studies only compared the results of

DES-treated and untreated biomass.<sup>28,36</sup> Thus, there is still a need to specify the advantages of DES pretreatment over conventional treatments.

**2.1.2 DESs as polymerization/crosslinking solvents.** DESs have shown their potential as media for polymerization/crosslinking reactions,<sup>51,52</sup> *e.g.*, the crosslinking of gelatin with epichlorohydrin in a DES composed of sodium acetate and urea,<sup>53</sup> the crosslinking of lactic acid (LA) with glycidyl methacrylate (GMA) in a DES composed of ChCl and LA,<sup>54</sup> and the polymerization of acrylic acid (AA) in liquid metal-added DES (ChCl and AA).<sup>55</sup> The polymerization/crosslinking reaction in DESs is more suitable for the biomass derivatives, not the raw biomass, which facilitates the synthesis of monolithic BCMS. For example, Ma *et al.* employed a Type III DES composed of ChCl, urea and glycerol (Gly) as the medium for the crosslinking of ethanol-fractionated kraft lignin with polyethylene glycol diglycidyl ether at 90 °C for 24 h.<sup>48</sup> After the replacement of the DES with ethanol and water, the resultant lignin hydrogel was carbonized and activated to prepare N-doped hierarchical porous carbon aerogel as high-efficient electrode material for electrochemical energy storage.<sup>48</sup> The authors mentioned that the DES could be recycled after a simple rotary evaporation. However, the recycled DES was not employed in the successive preparation of the carbon material. More efforts should be made to synthesize the functional monolithic BCMS based on the polymerization/crosslinking of biomass and its derivatives.

**2.1.3 DESs as solvents for electrospinning of biomass fiber.** Electrospinning emerges as a simple and versatile



process to engineer lignocellulosic biomass into nanofibers.<sup>56–58</sup> Conventionally, volatile organic solvents are used to dissolve polymers in electrospinning solutions. However, the conventional organic solvents always suffer from high toxicity, high flammability, and low dissolubility to biopolymers. Alternatively, emerging solvents, *e.g.*, ILs and DESs, are developed as high-efficiency solvents for the synthesis of fiber from biopolymers *via* electrospinning.<sup>56,59</sup> Benefiting from the merits of DESs toward ILs, DESs are more promising as substitutes for electrospinning.<sup>60,61</sup> Recently, owing to the high lignin solubility of acidic DESs, Rong *et al.* used ChCl-LA DES as the recyclable electrospinning solvent to prepare a lignin fiber aerogel (LFA) before the carbonization of the LFA (Fig. 2), and soluble linear polymer polyvinyl alcohol (PVA) was used as the linear template.<sup>59</sup> By controlling the amount of lignin and PVA in the DES, the resultant lignin fiber had an average diameter of 400 nm, and the resultant LFA showed a specific mass as low as 3 mg cm<sup>-3</sup> with a porosity >99.7%. Interestingly, in their strategy, the DES and PVA would be leached into water during the washing of lignin fiber, instead

of leaving in the lignin fibers.<sup>59</sup> Thus, DESs are promising as the solvents for wet electrospinning of biomass polymers to prepare nanofibers.

## 2.2 DES-mediated biomass carbonization for BCM preparation

### 2.2.1 STC of biomass in DESs.

Recently, STC using organic solvents, ILs, eutectic mixtures, and DESs for the preparation of carbon materials has progressed drastically as an alternative route to HTC in water, ascribed to the enhanced structures and properties of the resultant carbon materials from STC compared to those from HTC.<sup>12</sup> Tactlessly, in some cases, the carbonization of biomass using the above-mentioned solvents as media is still termed hydrothermal carbonization.<sup>62,63</sup> In addition, the carbonization using alcohol as medium is termed alcohothermal carbonization,<sup>64</sup> and the carbonization using ILs is termed ITC.<sup>19,65</sup> The application of DESs as the carbonization medium is developed from the solvothermal carbonization in organic solvents, ILs and eutectic mixtures, attributed to the various merits of DESs.

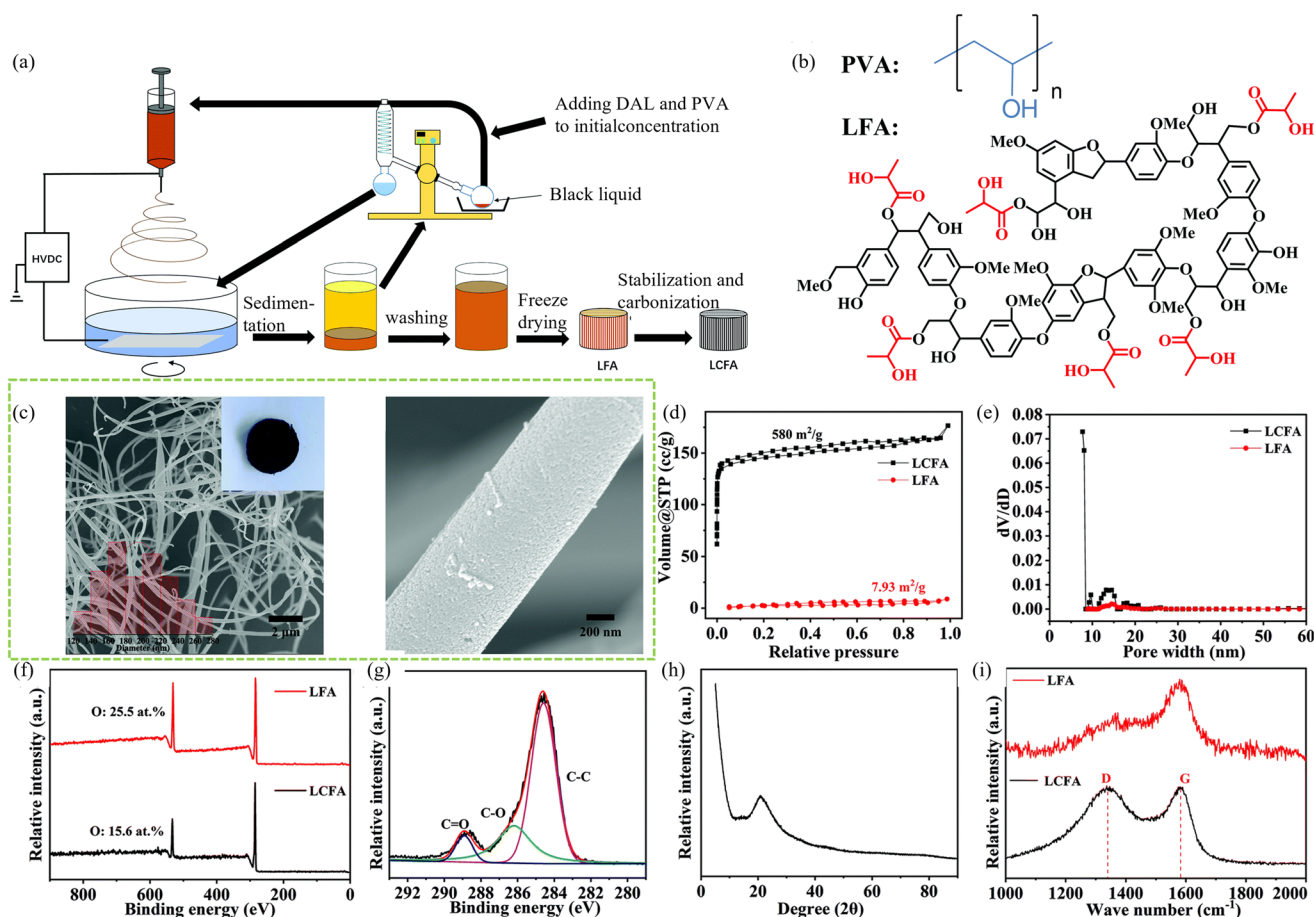


**Fig. 2** The fabrication of LFA and LCFA using the DES assisted no-waste electrospinning strategy and recycling process. (b) The PVA (blue) and hypothetical LFA (black and red) molecule. The red parts are the ester groups that reacted with lactic acid. (c) SEM images of LCFA. Insets in (a) are photographs of the LCFA and a graph showing the diameter distribution. (d) Nitrogen adsorption-desorption isotherm curves of LCFA and LFA. (e) Mesopore size distributions of LCFA and LFA. (f) XPS survey spectra of LFA and LCFA. (g) C 1s XPS spectrum of LCFA. (h) XRD curve of LCFA. (i) Raman spectra of LFA and LCFA.<sup>59</sup>



Table 2 BCMS prepared by the STC of biomass in DESs

Biomass	DESs	Carbonization conditions	BCMs	Application of BCMS	Ref.
1 Cotton stalk	ChCl + CA (1 : 1)	150–210 °C, 3 h	Carboxyl and phenol groups co-enriched BCM	U(vi) adsorption	23
2 Tea residue	ChCl + urea (1 : 1), (1 : 2), (1 : 3)	180–220 °C, 4–12 h	CDs	Cd detection	73
3 Chitin (shrimp shells)	ChCl + TsOH (3 : 1), (2 : 1), (1 : 1), (1 : 2), (1 : 3)	110 °C or 130 °C, 3 h	S/N/O co-doped carbon	Electrochemical energy storage	68
4 Hemicelluloses	ChCl + urea (1 : 1)	200 °C, 5–12 h	Nitrogen-doped hemicellulose-based carbon quantum dots (N–H–CQDs)	Ag <sup>+</sup> and L-cysteine fluorescent sensing	70
5 Hybrid poplar, Caribbean pine and corn stalk	ChCl + <i>p</i> -TsOH (1 : 1)	200 rpm, 140 °C, 1 h	High content of carbon and oxygen-containing functional groups	Cr(vi) adsorption	88
6 Lignin (wheat straw)	ChCl + LA (1 : 15)	180 °C, 6 h	Lignin CDs (LCDs)	Fe <sup>3+</sup> fluorescence sensing	45
7 Glucose	ChCl + EG + Glu (1 : 1 : 1)	180–220 °C, 5–15 h	Fe-doped carbon	Cationic pollutant adsorption Dye degradation catalyst Nitrobenzene to aniline catalysis	66
8 <i>Parthenium hysterophorus</i>	ChCl + FeCl <sub>3</sub> (1 : 2)	200 °C, 18 h	Tendrill-like carbon helices	Methylene blue, methyl orange adsorption	74
9 Glucose	ChCl + gly (1 : 2)	Microwave 350 W, 3 min	N, Cl-CDs	Co <sup>2+</sup> , Enrofloxacin fluorescent probe detection	75
10 Carob molasses	ZnCl <sub>2</sub> + EG (1 : 4) ChCl + EG (1 : 2) ChCl + urea (1 : 2) GL + LA (1 : 9)	300 °C, 1.25 h DES <sub>2</sub> 1 h	CDs	Antibacterial activity	72
11 <i>Parthenium hysterophorus</i>	ChCl + FeCl <sub>3</sub> (1 : 2)	200 °C, 18 h	Carbon helices	Enzyme host	24
12 Glucose	ChCl + EG (1 : 1)	180–220 °C, 5–15 h	Al-doped carbon	Water purification	71
13 Sewage sludge	ZnCl <sub>2</sub> + urea (1 : 3.5)	180–240 °C, 1 h	Low-N hydrochar		62
14 Garden waste	ChCl + H <sub>2</sub> O	160–260 °C, 3–9 h	Fe <sup>3+</sup> -catalyzed hydrochars	Methylene blue (MB) adsorption	63
15 AA	ChCl + EG (1 : 2)	180–220 °C, 3–12 h	Variable oxygen functionalities	Cyt-c enzymatic activity and stability acceleration	67

As shown in Table 2, a variety of biomass feedstocks, *e.g.*, glucose,<sup>66</sup> alginate,<sup>67</sup> shrimp shell,<sup>68</sup> sewage sludge,<sup>62</sup> DES-fractionated lignin,<sup>69</sup> hemicellulose,<sup>70</sup> and raw lignocellulosic biomass<sup>23</sup> have been applied for the preparation of BCMS through STC in various DESs. Among these biomasses, glucose can function as both the carbon precursor and DES component,<sup>26,66,71</sup> while other biomasses function as carbon precursors. Furthermore, the DES-mediated STC of biomass facilitates the preparation of BCMS in a variety of forms, *e.g.*, CDs,<sup>69,70,72,73</sup> carbon helices,<sup>24,74</sup> metal-doped carbon microspheres,<sup>66,71</sup> and carboxyl and phenol group co-enriched BCMS.<sup>23</sup> Besides the conventional heating of DESs, it is also worth noting that DESs have higher conductivities than water, facilitating their higher heating efficiency under microwave irradiation.<sup>75</sup> For example, Tabaraki and Nazari prepared CDs from glucose by microwave irradiation of the DES at 350 W for 3 min.<sup>75</sup> The process time for the preparation of CDs by microwave irradiation was much shorter than the that for the preparation of CDs from STC by conventional heating.<sup>75</sup> The application of a specific designer DES for the STC of biomass facilitates the specific physicochemical properties of the resultant BCM, *e.g.*, the carbon helices from the

leaves of *Parthenium hysterophorus*,<sup>24</sup> and the carboxyl and phenol groups co-enriched BCM from cotton stalk.<sup>23</sup> As shown in Fig. 3, Aruchamy *et al.* employed a Type II DES composed of ChCl and FeCl<sub>3</sub> (1 : 2 molar ratio) as the STC medium to prepare carbon helices from lignocellulosic biomasses (leaves of *Parthenium hysterophorus* and *Ricinus communis*).<sup>24</sup> Interestingly, they also found that cotton and silk were not suitable for the preparation of carbon helices under the same STC process.<sup>24</sup>

**2.2.2 Pyrolysis of biomass with DESs.** Besides the unconventional STC, conventional routes for the preparation of BCMS *via* pyrolysis could also be enhanced by the introduction of DESs to biomasses. For this route, DESs function as carbon precursors (*e.g.*, glucose as a HBD), heteroatom/metal dopants (*e.g.*, containing urea or metal chloride), soft templates, catalysts and/or activation agents (*e.g.*, containing ZnCl<sub>2</sub>) (Fig. 4).<sup>25,76–78</sup> Specifically, in 2016, Mondal *et al.* applied a ChCl–FeCl<sub>3</sub> DES as the template and catalyst for the conversion of pretreated seaweed (granules from the juice of *Sargassum tenerrimum*) at 700–900 °C into Fe<sub>3</sub>O<sub>4</sub>/Fe doped graphene-like carbon nanosheets as a high-efficiency electrocatalyst (Fig. 5).<sup>76</sup> Similarly, Ke *et al.* applied a Type IV DES (FeCl<sub>3</sub>–urea) as the iron and nitrogen dopant and activating



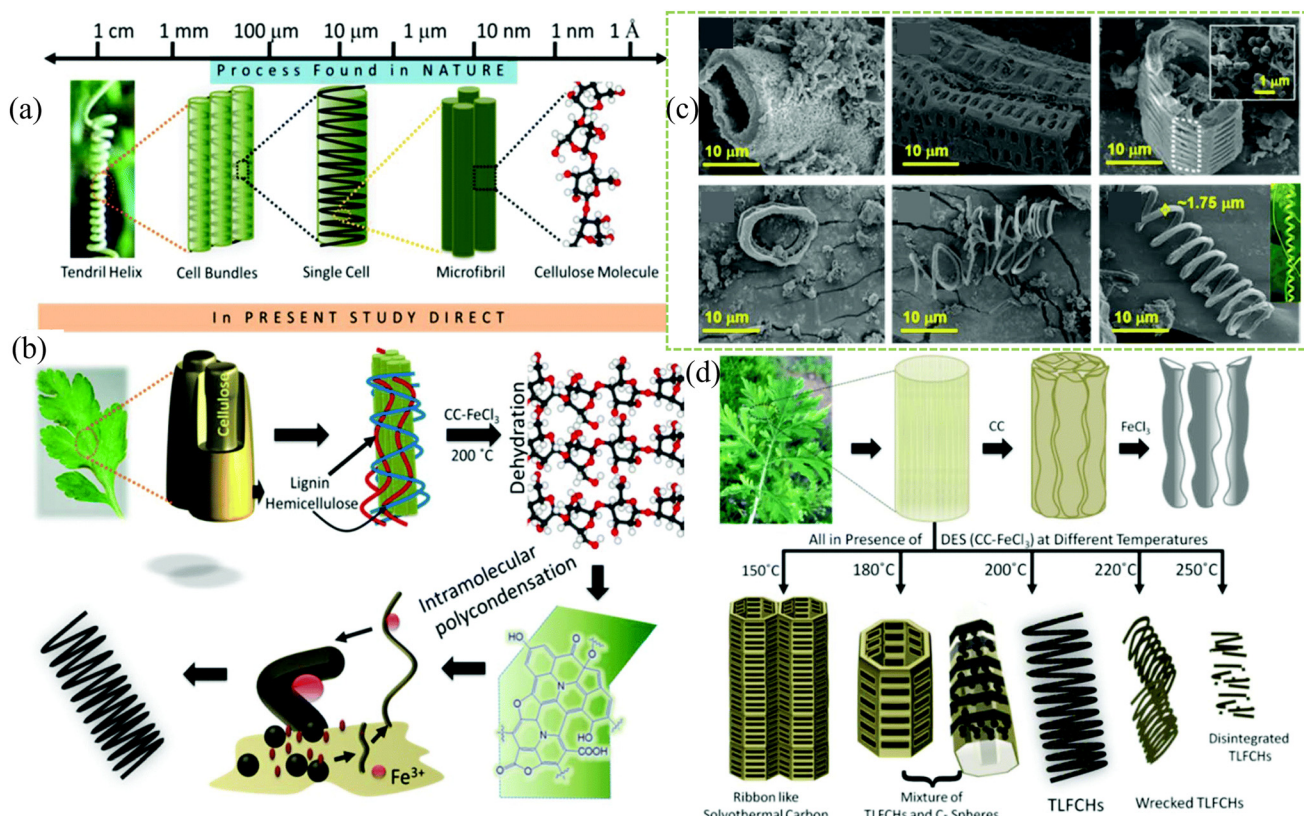


**Fig. 3** (a) hierarchical ordering of a tendril helix, successively built from bundles of cells containing cellulose found naturally in climbing plants. (b) A plausible mechanism of the sequential growth of TLFCHs from *Parthenium* biomass during a solvothermal process in the presence of a DES. (c) Field emission scanning electron microscopy images of *Parthenium hysterophorus* derived solvothermal carbons. (d) Schematic representation of biomass conversion to different morphologies during the hydrothermal/solvothermal process under different reaction conditions.<sup>24</sup>

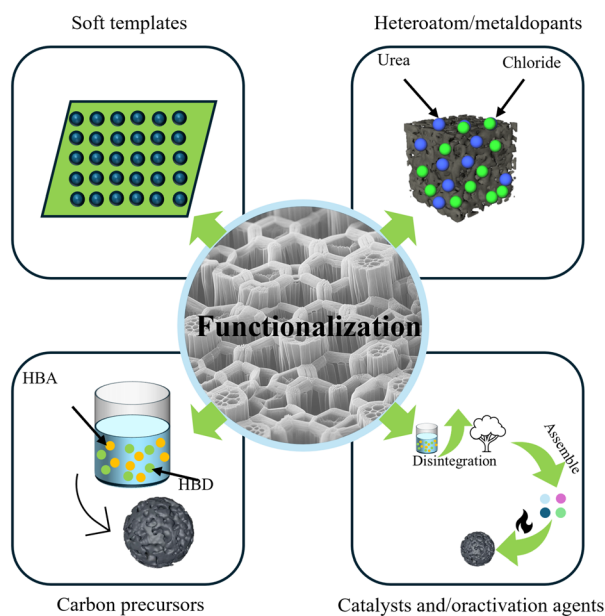


**Fig. 4** The DES-mediated pyrolysis of biomass for the preparation of BCMS.

agent for the preparation of a nitrogen-doped magnetic porous BCM from peanut shell.<sup>79</sup> Chen *et al.* also employed a ChCl-ZnCl<sub>2</sub> DES as the nitrogen-doping catalyst (ZnCl<sub>2</sub> as a Lewis acid to catalyze the substitution of phenol groups by amines) and activation agent for the preparation of nitrogen-doped nanoporous carbon from lignin by pyrolysis of a mixture of lignin, urea, and ChCl-ZnCl<sub>2</sub> DES at 700 °C.<sup>77</sup> However, the results from Chen *et al.* lacked a comparison of the resultant carbon material from that obtained by the pyrolysis of the mixture of lignin, urea and ZnCl<sub>2</sub>.<sup>77</sup> Thus, it is still unclear whether there is an advantage of the ChCl-ZnCl<sub>2</sub> DES in the preparation of nitrogen-doped porous carbon over conventional routes.<sup>77</sup>

DESs have been observed to be efficient in enhancing the formation of a cellulose nanofiber (CNF) aerogel by improving hydrogen bonding interaction.<sup>25</sup> For example, Long *et al.* applied a ChCl-glucose DES to enhance the hydrogen-bonding of a CNF aerogel for the preparation of a CNF carbon aerogel.<sup>25</sup> They found that the resultant CNF carbon aerogel showed a smooth surface when no DES was used for the formation of the CNF aerogel, while a rough surface was obtained for the DES-assisted CNF carbon aerogel, suggesting that the enhanced hydrogen-bonding by the DES might facilitate the



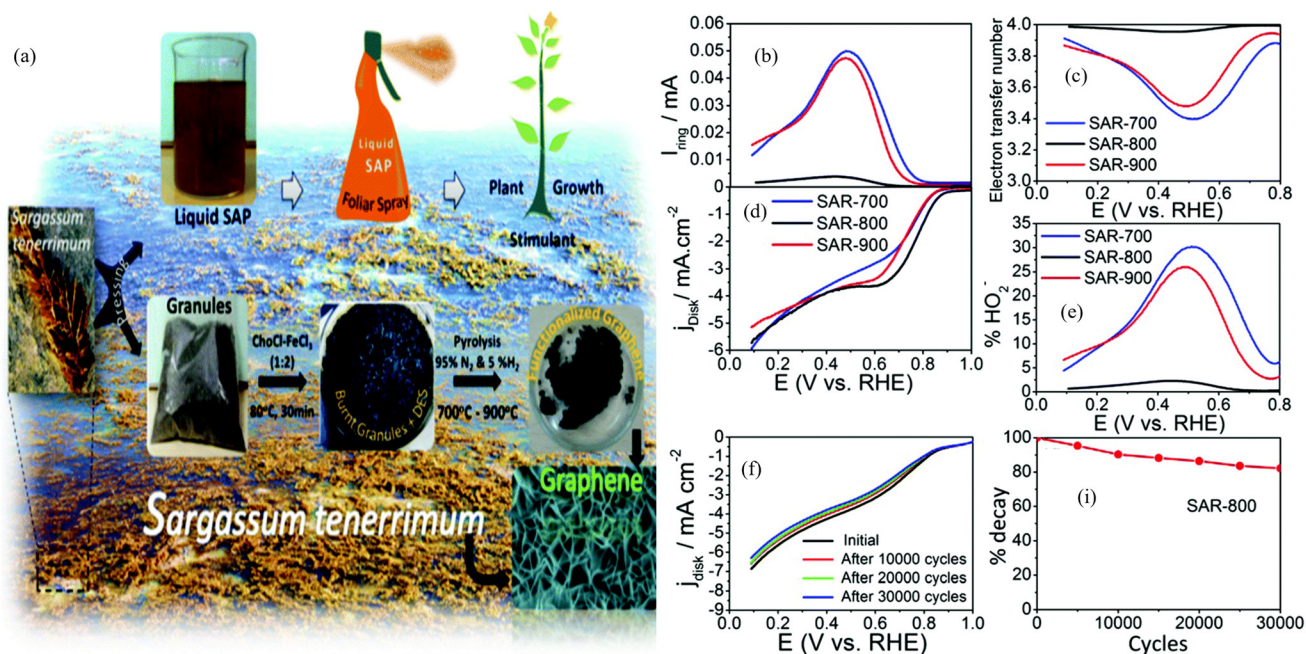


**Fig. 5** (a) The production of magnetite functionalized graphene from *Sargassum tenerrimum*. (b) Ring current as a function of electrode potential. (c) The electron transfer number for Fe/graphene composites as a function of electrode potential. (d) The rotating ring-disk electrode (RRDE) test of the ORR on magnetite-doped GNs in an oxygen saturated 0.1 M KOH alkali solution at 1600 rpm. (e) Peroxide percentage as a function of electrode potential. (f) Stability test conducted on SAR-800. (i) % Decay of the catalyst calculated for the number of cycles using stability test data.<sup>76</sup>

preservation of the morphology of the CNF aerogel.<sup>25</sup> In addition, other DESs, such as ChCl–organic acid and ChCl–alcohol, were also observed to be as efficient as the ChCl–glucose DES in the preparation of a high-performance CNF carbon aerogel.<sup>25</sup>

DESs have also been applied as the carbon precursor and self-templates for BCM preparation.<sup>80,81</sup> Specifically, a biomass derivative-based ternary DES composed of ChCl, urea and gluconic acid was converted into Co nanoparticle-supported nitrogen-doped porous carbon (Co@NPC) by mixing the DES with  $\text{Co}(\text{NO}_3)_2$ , followed by freeze-drying and pyrolysis at  $700$ – $900^\circ\text{C}$ .<sup>78</sup> The results by Li *et al.* further indicated that the ternary DES was more favorable for enhancing the performance of the resultant material.<sup>78</sup> However, these results still showed a lack of the advantages of the biomass derivative-based ternary DES over the route without a DES for the preparation of functional BCMs.<sup>78</sup>

### 2.3 DESs for the post-functionalization of BCMs

**2.3.1 Impregnation of BCMs with DESs.** Recently, a variety of porous carbons have been impregnated with DESs for enhancing  $\text{CO}_2$  capture.<sup>30,31,82,83</sup> Specifically, Ariyanto *et al.* conducted the impregnation of a DES on a porous BCM by vacuum impregnation of the mixture of DES and porous BCM (1 : 1 weight/volume) at a pressure of  $-0.5$  bar, followed by drying of the slurry at  $105^\circ\text{C}$  for 20 h.<sup>31</sup> Ultrasonication has also been applied to conduct the DES impregnation on the BCM. For example, Hussin *et al.* conducted the DES impregnation by thoroughly mixing the DES with the porous BCM at

a 2 : 1 ratio, followed by stirring at  $65^\circ\text{C}$  for 2 h under ultrasonication, washing, filtering and drying.<sup>30</sup> Besides the DES-impregnation of porous BCMs,<sup>30–32,82–84</sup> DES impregnation has also been applied to enhance the performances of clay-composited BCMs and magnetic BCMs toward pollutant adsorption.<sup>85,86</sup>

**2.3.2 Solvothermal treatment of BCM in DESs.** In addition to the simple impregnation of DESs onto a BCM, the post-modification of the BCM could also be conducted under solvothermal conditions, *i.e.*, heating the BCM in DESs in an autoclave. Ye *et al.* proposed this strategy to synchronously separate fibrils from the BCM from *Ramie* filaments and dope nitrogen on the surface of the BCM.<sup>87</sup> Specifically, the raw BCM from *Ramie* filaments was soaked into a ChCl–urea DES at a solid–liquid ratio of 1 : 100, and then treated at  $120^\circ\text{C}$  for 12 h. The BCM after solvothermal treatment in the DES was calcined at  $900^\circ\text{C}$  in  $\text{N}_2$  to obtain the nitrogen-doped BCM for catalytic degradation of pollutants in solution.<sup>87</sup> Their results showed that the solvothermal treatment of the raw BCM in the ChCl–urea DES was more efficient than the direct impregnation of urea for the preparation of a nitrogen-doped BCM as a catalyst for pollutant degradation. The advantages of DES-mediated modification of the BCM over conventional urea impregnation might be ascribed to the synchronous separation of the fiber structure and doping of nitrogen on the resultant BCM during solvothermal treatment in the ChCl–urea DES, while the direct urea impregnation only has an impact on nitrogen-doping.<sup>87</sup>



### 3. Types of BCMs prepared or functionalized by the involvement of DESs

With the favor of DESs, a variety of BCMs have been developed, including CDs, carbon aerogels, porous BCMs, composited BCMs, carbon helices, and surface functionality-enriched BCMs (Fig. 6).

#### 3.1 CDs

CDs, as a rising star of emerging zero-dimensional carbon nano-materials, have attracted considerable attention for versatile applications, attributed to their promising properties, such as superior optical and electrical properties, high quantum yield, excellent photostability, high biocompatibility and low toxicity.<sup>89,90</sup> Biomass is a promising sustainable carbon source for the synthesis of CDs.<sup>90</sup> Recently, HTC,<sup>91</sup> pyrolysis,<sup>92</sup> microwave irradiation,<sup>93</sup> chemical oxidation and ultrasonication have been developed for the synthesis of CDs from biomass. Similarly, direct low temperature pyrolysis,<sup>72</sup> STC,<sup>73</sup> and microwave irradiation<sup>75</sup> were employed for the DES-mediated synthesis of CDs from various biomasses, including glucose,<sup>72,75</sup> hemicellulose,<sup>70</sup> DES-fractionated lignin from wheat straw,<sup>45</sup> DES-extracted soluble fraction from bamboo,<sup>94</sup> and tea residue.<sup>73</sup>

It is well noted that the CD properties are controlled by the chemical composition of carbon sources, and the type of passivation agent for the conventional CD synthesis routes. Calhan *et al.* observed that CDs obtained from water, ZnCl<sub>2</sub>-EG DES, ChCl-EG DES, ChCl-urea DES, and glycine-LA DES showed different properties, such as surface functional groups and optical, fluorescence and electronic properties.<sup>72</sup> Thus, for the DES-mediated synthesis of biomass CDs, the properties of CDs can be tuned by the composition of DESs.<sup>72</sup>

#### 3.2 Carbon aerogels

Carbon aerogels are a class of carbon materials with 3D networked structures.<sup>95</sup> Besides the well-known organic polymer, graphene and CNTs, biomass has also been proposed as an inexpensive, abundant and sustainable precursor to prepare carbon aerogels.<sup>96</sup> For the synthesis of biomass-derived carbon aerogels, DESs can function as solvents, carbon precursors and/or surface modification agents.<sup>25,48,59</sup> The formation of a biomass aerogel is vital for the subsequent synthesis of a carbon aerogel *via* a carbonization process. DESs are attractive solvents for the preparation of aerogels owing to their strong H-bond networks, enhancing the 3D networked structures.<sup>25</sup> It has been observed that the CNF carbon aerogel remarkably changed from hydrophilic to hydrophobic (with a water contact angle from <1° to around 130°) with the assistance of the ChCl-glucose DES in the DES-CNF aerogel.<sup>25</sup> Besides CNF, a lignin-derived carbon aerogel can also be synthesized with the assistance of DESs as the solvent for crosslinking of lignin with poly(ethylene glycol) diglycidyl ether (PEGDE)<sup>48</sup> and the solvent for electrospinning of lignin fiber.<sup>59</sup>

#### 3.3 Porous BCMs

Recently, porous BCMs derived from DES-pretreated biomass, from co-pyrolysis of biomass with a DES, and post-treated with the DES, were developed. For these porous BCMs, DESs function as pretreatment solvents, activation agents, heteroatom dopants, and/or surface modification agents. However, the advantages of DESs in the biomass pretreatment for porous BCM preparation are still unclear, attributed to the lack of direct comparisons with convention solvents.<sup>28,36</sup>

#### 3.4 Composited BCMs

The DES-mediated BCM composites can be directly prepared by the STC of biomass in metal salt-containing DESs,<sup>66,71</sup> or pyrolysis of a mixture of biomass and metal salt-containing DES.<sup>76,78,79</sup> For example, Halanur *et al.* prepared Fe<sub>2</sub>O<sub>3</sub>-doped carbon microspheres by the STC of an FeSO<sub>4</sub>-added ChCl-glucose-EG DES,<sup>66</sup> and Mondal *et al.* prepared Fe<sub>3</sub>O<sub>4</sub>/Fe doped carbon nanosheets by the pyrolysis of a mixture of seaweed-derived extracts and ChCl-FeCl<sub>3</sub> DES.<sup>76</sup> In addition, DES-mediated BCM composites also can be prepared by using DESs as treatment solvents, as solvents for doping of metal species, or as post-modification agents.

#### 3.5 Carbon helices

The precise morphology control is also important for the application of the resultant BCMs. The preparation of carbon helices is always a high energy-consuming, chemical-intensive, and multi-step process.<sup>74,97</sup> By the STC of the leaves of *Parthenium hysterophorus* in a DES composed of ChCl and FeCl<sub>3</sub> at around 200 °C, Aruchamy *et al.* obtained tendril-like carbon helices.<sup>24</sup> However, little is known about the selectivity to the DES composition and biomass feedstock for the preparation of carbon helices. More efforts are needed to elucidate the roles of the ChCl-FeCl<sub>3</sub> DES and the biomass feedstock on the morphology of the resultant helices.

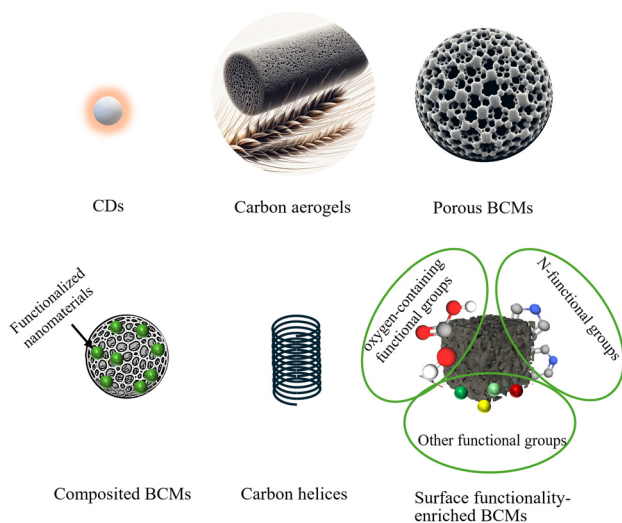


Fig. 6 Types of BCMs prepared or functionalized by the involvement of DESs.



### 3.6 Surface functionality-enriched BCMs

It has been well observed that STC in DESs facilitates the enrichment of the surface functionality of the resultant BCM. <sup>24,63,66,67,88</sup> For example, Lai *et al.* observed that the BCM prepared by the STC of corn stover in a ChCl-CA DES showed much richer contents of carboxyl and phenol groups than the BCM prepared by conventional HTC, <sup>23</sup> and Yadav *et al.* observed that the BCM prepared by the STC of alginic acid in a ChCl-EG DES was also remarkably richer in oxygenated functional groups (OFGs) than the BCM prepared by HTC in water. <sup>67</sup> The enrichment of surface functionality on the resultant BCM by STC in the DES is also tuned by the components of the DES. For example, besides the enrichment of OFGs, the STC of shrimp shell in the DES composed of ChCl and *p*-toluenesulfonic acid monohydrate (TsOH) enriched the sulfur content in the resultant BCM. <sup>68</sup>

## 4. Applications of BCMs mediated by DESs

### 4.1 Adsorption/separation

**4.1.1 Gas adsorption/separation.** DESs have been considered as green absorbents for gases (*i.e.*, CO<sub>2</sub> and SO<sub>2</sub>). <sup>98</sup>

For example, Mohan *et al.* predicted the CO<sub>2</sub> capture ability of DESs using quantum chemistry and machine learning, which was critical for the preparation of designer DESs for CO<sub>2</sub> capture. <sup>98</sup> In addition, porous carbon is also commonly used for CO<sub>2</sub> capture. Consequently, the combination of DESs and porous carbon has attracted attention for CO<sub>2</sub> capture. Recently, Ariyanto *et al.*, Hussin *et al.*, and Mukherjee *et al.* impregnated porous carbons with DESs to enhance their CO<sub>2</sub> capture performances. <sup>30,31,83</sup> Specifically, the results from Ariyanto *et al.* showed that, although the specific surface area for DES-impregnated porous carbon decreased by 67%–73%, its CO<sub>2</sub> capture capacity increased up to 1.6 times at 1 atm and 30 °C, and the selectivity of CO<sub>2</sub>/CH<sub>4</sub> also increased to 125%. <sup>31</sup> A higher CO<sub>2</sub> adsorption capacity of 37.2 mg g<sup>-1</sup> was achieved by Hussin *et al.* <sup>30</sup> They observed that a choline hydroxide (ChOH)-urea DES as the impregnation solvent increased the CO<sub>2</sub> adsorption capacity of palm shell-derived porous carbon from 6.5 to 37.2 mg g<sup>-1</sup> at 25 °C (Fig. 7a and b). <sup>30</sup> In addition, DES-impregnated porous carbon has also shown enhanced performance in SO<sub>2</sub> adsorption. <sup>99</sup> The significant increase in CO<sub>2</sub> and SO<sub>2</sub> adsorption by DES impregnation might be ascribed to the enhanced H-bonding, charge transfer, and acid-based interactions. <sup>31,99</sup>

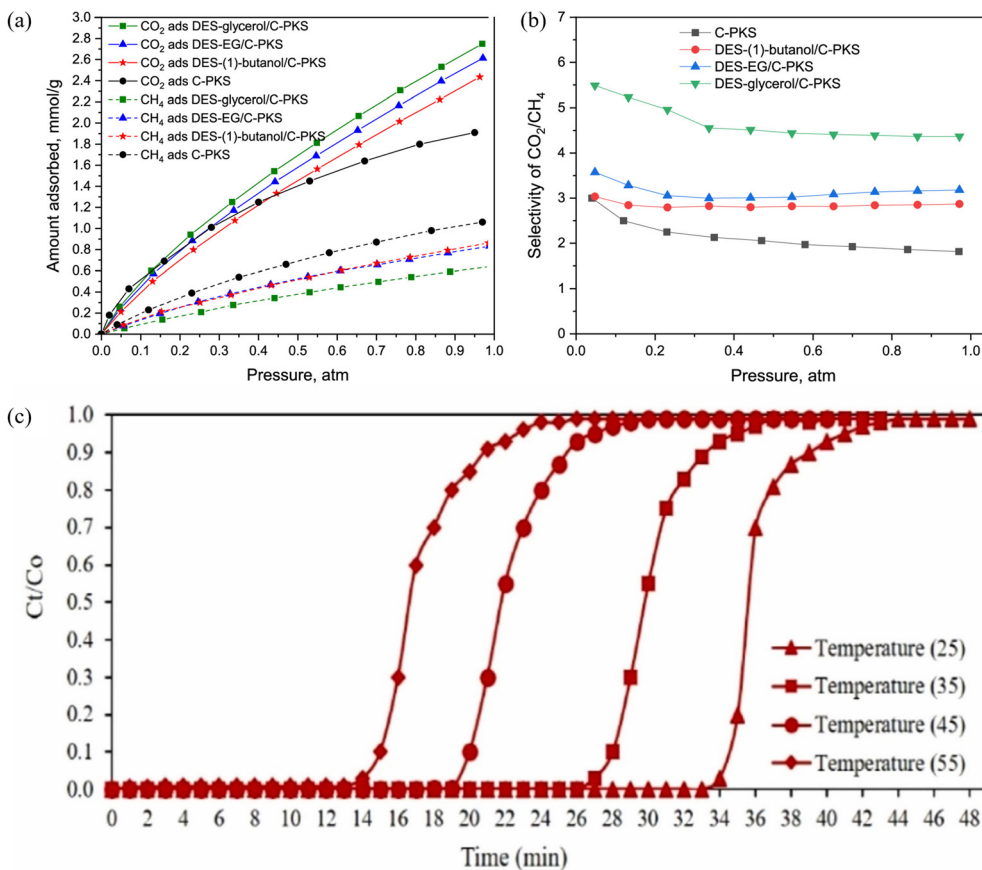


**Fig. 7** (a) Adsorption isotherm of CO<sub>2</sub> and CH<sub>4</sub> using DES/porous carbons and the reference of porous carbon. (b) Selectivity of CO<sub>2</sub>/CH<sub>4</sub> based on the ratio of adsorption uptake. (c) Effect of adsorption temperatures on CO<sub>2</sub> adsorption ACDES 9:  $\Delta$  25 °C,  $\square$  35 °C,  $\circ$  45 °C and  $\diamond$  55 °C (reaction conditions: gas flow rate = 200 mL min<sup>-1</sup>; initial CO<sub>2</sub> concentration = 10%). <sup>30</sup> With permission. Copyright 2021 Elsevier.



**4.1.2 Pollutant adsorption from solution.** A variety of BCMs, including the BCMs synthesized by the STC of biomass in DESS<sup>24,45,63,71</sup> and pyrolysis of biomass with DESS,<sup>26,78,100–102</sup> and functionalized by the impregnation of a pristine BCM with a DES, have been developed for the adsorption of heavy metals,<sup>71,79,88</sup> dyes,<sup>63,66,74</sup> antibiotics,<sup>71,85</sup> drugs<sup>86,103</sup> and surfactants<sup>71</sup> from solutions. These BCMs demonstrated excellent properties in the adsorption and reduction of heavy metals (*i.e.*, Pb, Cr(vi) and U(vi)).<sup>23</sup> The effectiveness of the BCM is largely attributed to its rich surface functional groups.

The surface of the BCM, enriched with carboxyl and phenolic hydroxyl groups, has a high affinity for binding with U(vi),<sup>104</sup> thereby enhancing its capacity to adsorb U(vi) from wastewater. Consequently, producing a BCM enriched with these groups presents a practical and reliable approach for treating uranium-contaminated wastewater. For example, as shown in Fig. 8 the STC prepared by Lai *et al.*, using a DES composed of ChCl and CA as the STC medium, has a much higher content of phenolic hydroxyl and carboxyl groups compared to traditional hydrothermal carbon. The resultant bio-carbon prepared at 180 °C for 3 h achieved an adsorption capacity of 353 mg g<sup>-1</sup> for U(vi), and had a robust recyclability.<sup>23</sup>

BCMs have also demonstrated excellent performance for Cr(vi) removal. For example, Ke *et al.* prepared a nitrogen-doped magnetic BCM by co-pyrolysis of peanut shell with a urea-FeCl<sub>3</sub> DES,<sup>79</sup> and Zhang *et al.* prepared a BCM by the STC of wood biomass in a ChCl-TsOH DES for Cr(vi) removal.<sup>88</sup>

Specifically, the BCMs prepared by Zhang *et al.* achieved an adsorption efficiency of 270.3 mg g<sup>-1</sup> for Cr(vi). The better Cr(vi) adsorption performance by the BCM prepared by Zhang *et al.* suggests that the surface organic functional groups on BCMs are more important for Cr(vi) adsorption (Fig. 9a and b).<sup>79,88</sup>

Additionally, Pam *et al.* have prepared porous carbon using a DES and phosphoric acid as activation agents. This porous carbon possesses an excellent porous structure and a large specific surface area. Its maximum adsorption capacity for Pb(II) is 62.8 mg g<sup>-1</sup> and thermodynamic analysis has indicated that the adsorption process is exothermic and spontaneous (Fig. 9c and d).<sup>102</sup>

In addition to the adsorption of heavy metals, other organic pollutants such as dyes, pharmaceutical waste, and phenolic surfactants can also be adsorbed and degraded by the BCMs produced with the favor of DESS.<sup>63,66,74,85,86,103</sup> Specifically, Manohara *et al.* first prepared a eutectic system (ES) by combining ethylene glycol (EG), glucose, and ChCl in a molar ratio of 1:1:1. They then added aluminum nitrate hydrate and processed it at various STC temperatures and durations to produce BCMs enriched with surface OFGs. The resulting BCMs, which exhibited spheroidal or multi-spherical assemblies, were fabricated into membranes to investigate their adsorption effects on various pollutants. Their results demonstrated that besides negatively charged dyes (with an Eriochrome Black T rejection of 27.7%), positively charged dyes (MG and MB) achieved a rejection rate of 99.9%, effectively reaching complete removal. The

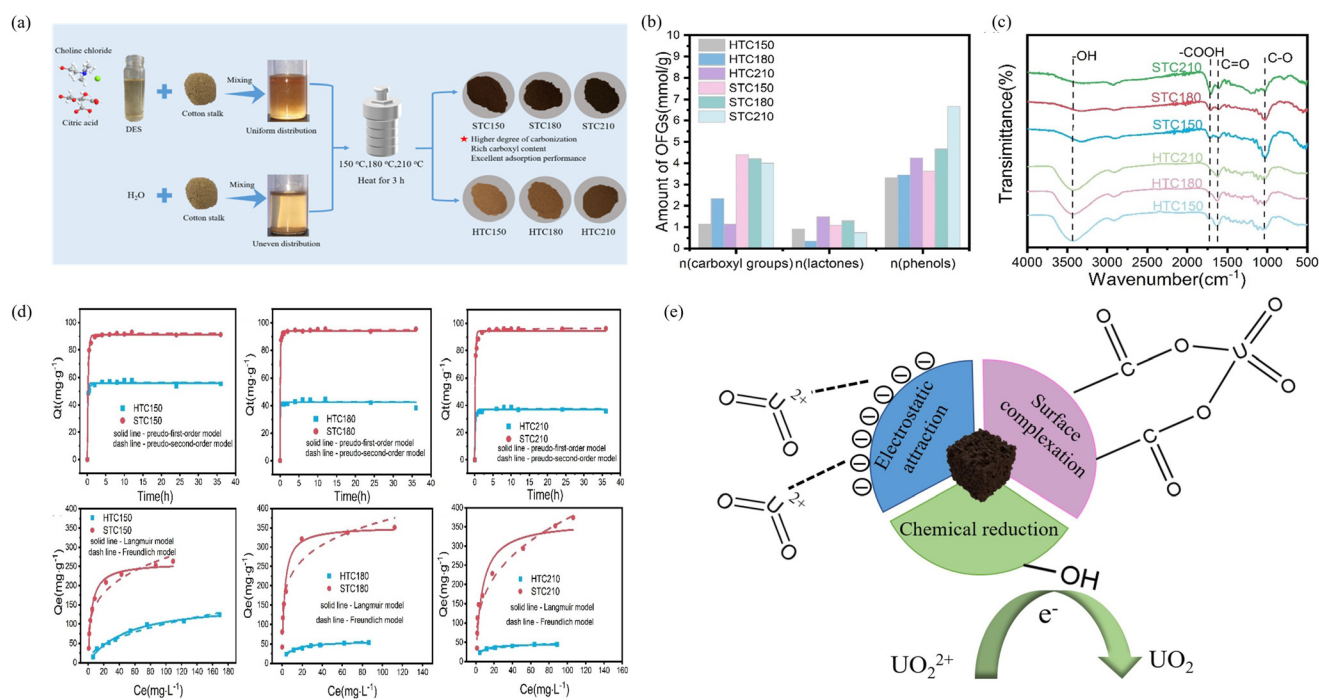


**Fig. 8** (a) Synthesis schematic of HTCs and STCs. (b) Contents of oxygen-containing functional groups of HTCs and STCs. (c) FTIR spectra. (d) The adsorption kinetics and adsorption isotherms of HTCs and STCs. (e) The adsorption mechanism of U(vi) on STCs.<sup>23</sup> With permission. Copyright 2023 Elsevier.



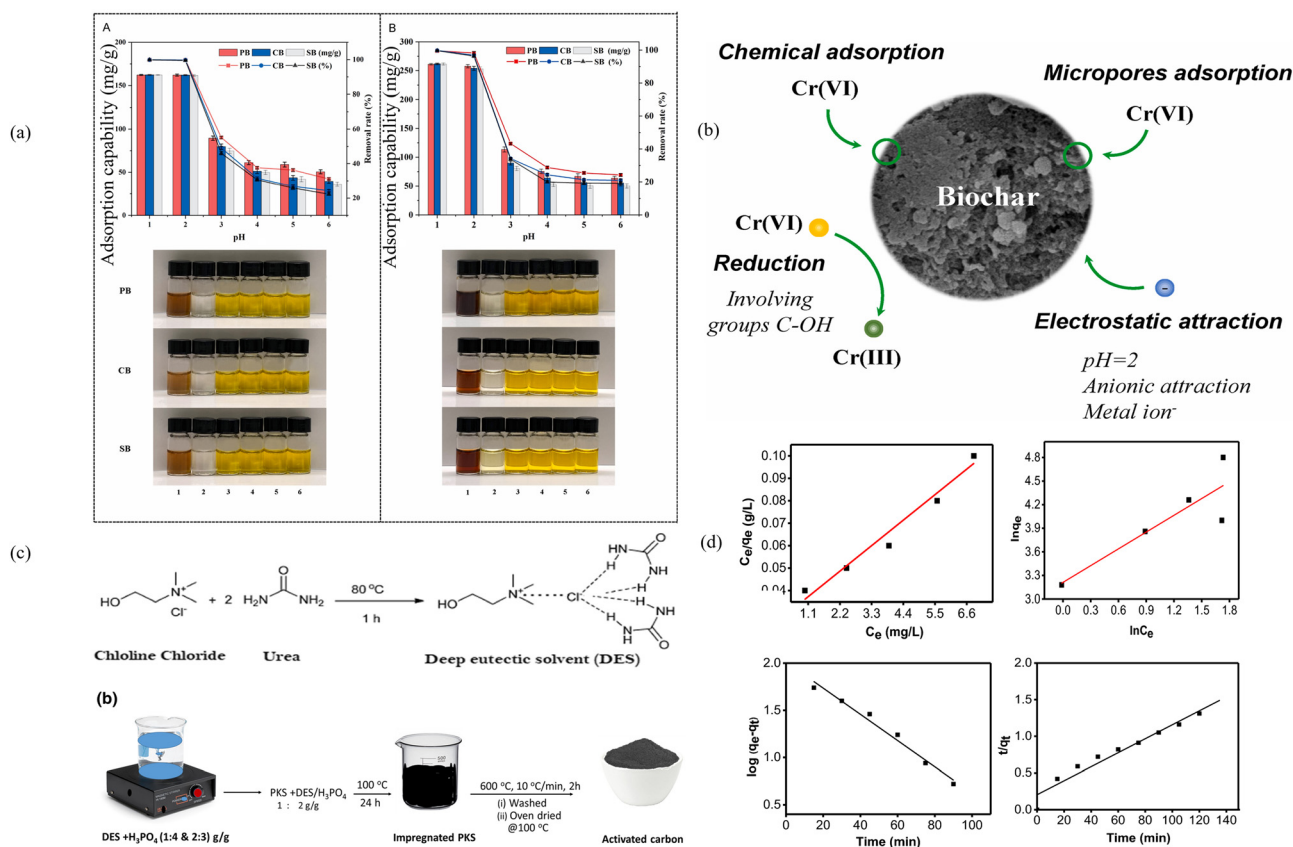


**Fig. 9** (a) Effect of pH on the adsorption properties of the BCM. (A) The initial concentration of Cr(vi) is 325.0 mg L<sup>-1</sup>; (B) the initial concentration of Cr(vi) is 525.0 mg L<sup>-1</sup>; the dosage of the BCM was 0.05 g, and the temperature was 30 °C; the volume of the solution was 25 mL. (b) Schematic mechanism diagram of Cr(vi) removal using biochar.<sup>88</sup> With permission. Copyright 2021 Elsevier. (c) Synthesis route of the DES/H<sub>3</sub>PO<sub>4</sub> based adsorbent. (d) Adsorption isotherm model of Pb(II) adsorption.<sup>102</sup>

materials also showed significant removal efficiency for ciprofloxacin and were capable of removing a substantial portion of some hormones and surfactants, with oxytocin and CTAB removal rates at 88.6% and 94.9%, respectively (Fig. 10).<sup>71</sup> Besides the preparation of the BCM through the direct STC of a DES (as the carbon precursor),<sup>66,71</sup> the BCM prepared by direct pyrolysis of a glucose-containing DES,<sup>103</sup> the BCM modified by solvothermal treatment of biochar in a DES,<sup>105</sup> the BCM functionalized by impregnation of magnetic porous carbon with a ChCl–Gly DES,<sup>86</sup> the BCM prepared by successive STC of biomass in a DES and physical activation,<sup>74</sup> and the BCM prepared by the STC of biomass in a DES<sup>63</sup> were developed for the adsorption of organic pollutants. However, some of these applications were not competitive compared to the existing adsorbents. The necessity for using DESs for the preparation or functionalization of BCMs is questionable.

**4.1.3 Oil–water separation.** DESs hold immense potential for achieving environmentally friendly oil–water separation. An example of this is the work of Long *et al.*, who utilized a DES composed of ChCl and glucose in combination with a CNF solution from eucalyptus pulp. At a relatively low pyrolysis temperature of 350 °C, they successfully prepared a carbon

aerogel. This aerogel demonstrated an impressive absorption capacity for oil and organic solvents, ranging from 74.1 to 95.2% (v/v), which is comparable to the effectiveness of general high-capacity adsorbent materials. Additionally, the adsorbed substances could be repeatedly recovered through distillation, with the aerogel maintaining high stability for up to 100 cycles (Fig. 11).<sup>25</sup>

**4.1.4 Capacitive deionization.** Carbon materials are extensively studied as electrode materials for capacitive adsorption.<sup>106,107</sup> However, typical carbon electrodes face challenges such as weak ion binding strength, high resistance, and poor capacitance, which hinder further development. DESs, with their ability to introduce rich functional groups and enable nitrogen doping, have attracted widespread attention for improving the advantages of ordinary carbon materials. Arangadi *et al.* embedded a ChCl–urea DES into AC to enhance the electro-adsorptive performance in CDI applications.<sup>108</sup> Their results suggested that although DES-embedded AC had a nearly 55% reduction in micropore surface area and a 33.96% reduction in specific capacitance at a scan rate of 10 mV s<sup>-1</sup>, the electro-adsorption capacity was remarkably increased from 15.45 to 28.60 mg g<sup>-1</sup>, with an 85% improvement in the electro-adsorption capacity (Fig. 12).<sup>108</sup> Additionally, the rate



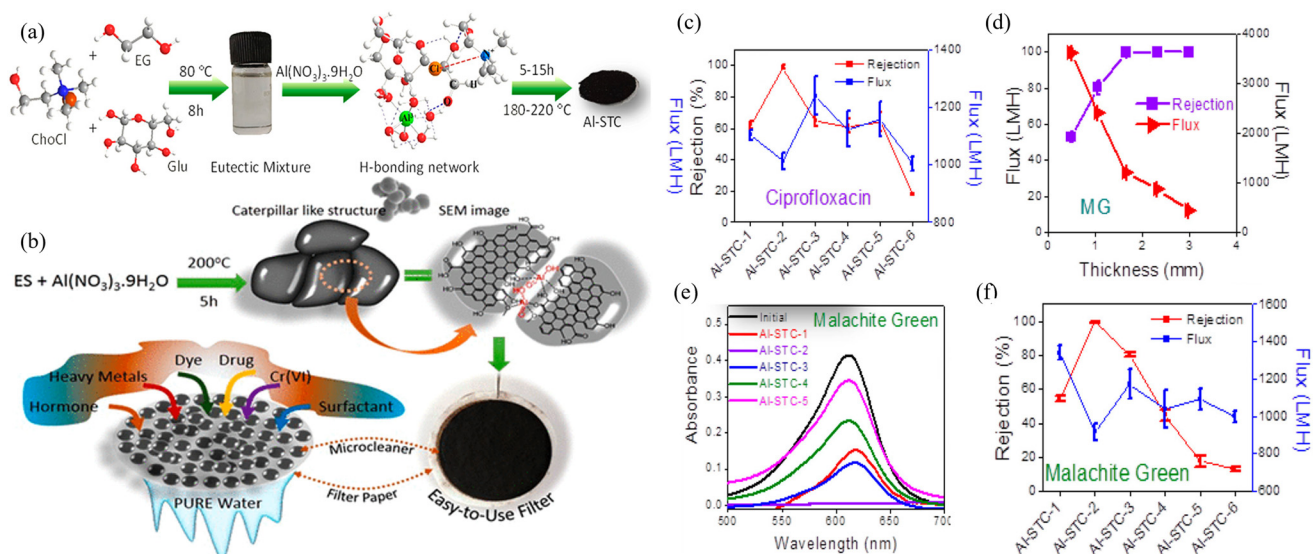


**Fig. 10** (a) Schematic of the synthesis of Al-STCs from a glucose based eutectic system. (b) The protocol followed in the whole process to purify the contaminated water from the Al-STC-2 material. (c) The flux and rejection of ciprofloxacin obtained using prepared Al-STC membranes. (d) The flux and rejection with respect to the thickness of the membrane for MG dye (e and f) the flux and rejection of MG obtained using prepared Al-STC membranes and the respective UV graph.<sup>71</sup> With permission. Copyright 2019 American Chemical Society.

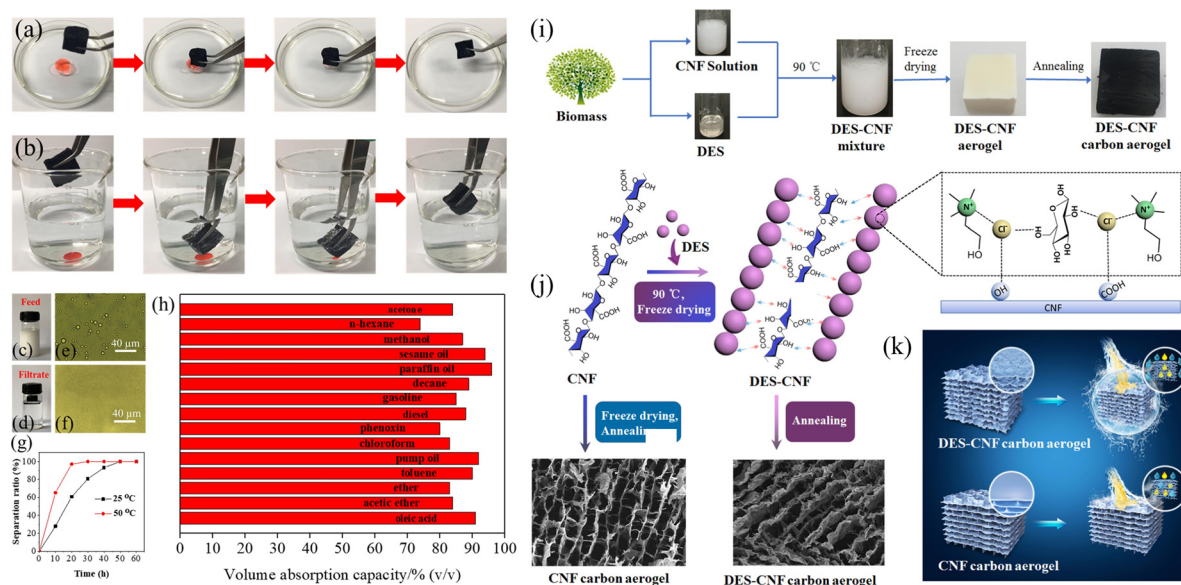


**Fig. 11** (a and b) Absorption of pump oil from water and CCl<sub>4</sub> from under water. (c–e) Photographs of the water-in-toluene emulsion before and after separation. (d–f) The optical microscopy images of the water-in-toluene emulsion before and after separation. (g) Absorption kinetics of DCCA-350 at 25 °C and 50 °C. (h) Absorption efficiency of DCCA-350 for various organic liquids. (i) The synthetic process of the DES carbon aerogel. (j) The bonding mechanism between the CNF and DES. (k) A hydrophobic DCCA-350 sample and a hydrophilic CNF carbon aerogel.<sup>25</sup> With permission. Copyright 2021 Elsevier.

of electro-adsorption and the cycle of charge and discharge were also significantly improved.<sup>108</sup>

## 4.2 Catalysis

**4.2.1 Catalytic degradation of pollutants.** BCMS feature an abundance of persistent free radicals and surface functional groups, enabling the generation of free radicals even without

the addition of oxidants. The addition of oxidants such as peroxodisulfate (PDS) allows the BCM to activate them, producing reactive oxygen species (ROS), singlet oxygen (<sup>1</sup>O<sub>2</sub>), hydroxyl radicals (<sup>•</sup>OH), and sulfate radicals (SO<sub>4</sub><sup>•-</sup>). These free radicals can effectively degrade organic pollutants such as tetracycline, phenol, and umifenovir.<sup>109–111</sup> The incorporation of nitrogen (N) into the BCM by the solvothermal treatment of ramie fiber-



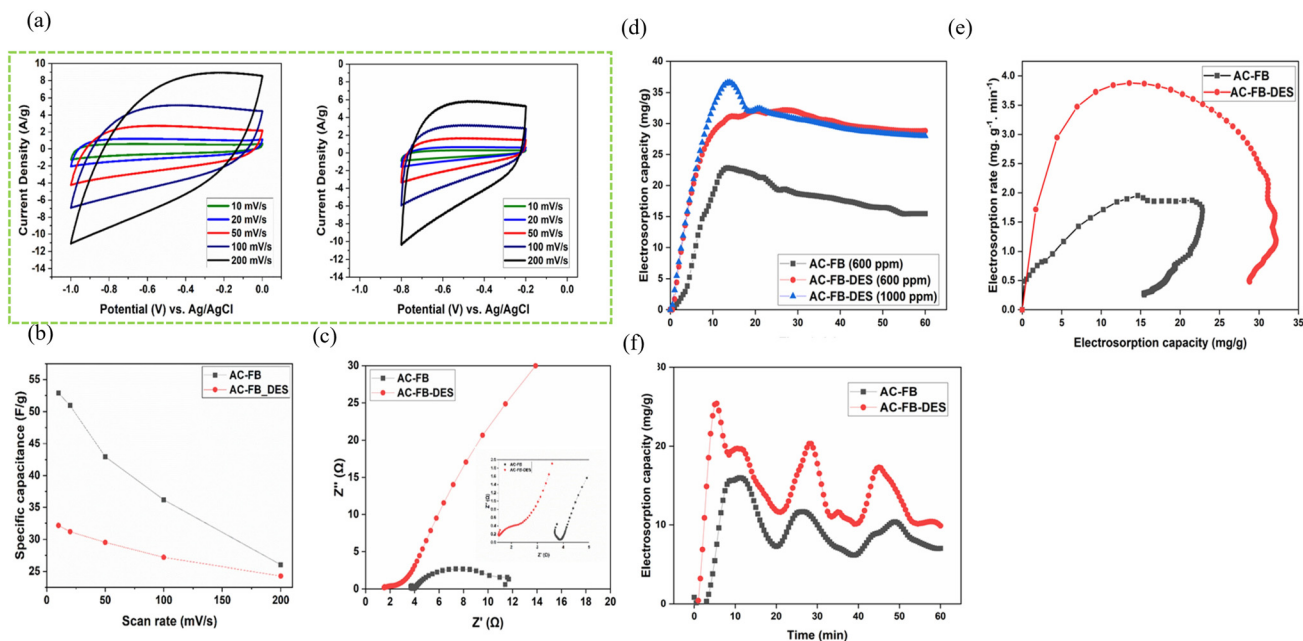


**Fig. 12** (a) Voltammogram of different carbon materials. (b) Variation of specific capacitance with the scan rate. (c) Nyquist plots for both AC-FB and AC-FB-DES electrodes. (d) Electrosorption capacity for AC-FB and AC-FB-DES on NaCl solution at 1.2 V. (e) Electrosorption rate for AC-FB and AC-FB-DES on 600 ppm NaCl solution in the CDI cell. (f) Charge–discharge cycle (10 min charge–10 min discharge cycle) for AC-FB and AC-FB-DES on 600 ppm NaCl solution in the CDI cell.<sup>108</sup> With permission. Copyright 2022 Elsevier.

derived biochar in the ChCl–urea DES at 120 °C for 12 h increased the catalytic degradation rate constant for tetracycline from  $0.0051 \text{ min}^{-1}$  to  $0.0221 \text{ min}^{-1}$ . It is worth noting that the ChCl–urea DES-based solvothermal doping of nitrogen into the ramie fiber-derived biochar outperformed the nitrogen-doped biochar functionalized by re-pyrolysis of the ramie fiber-derived biochar with urea.<sup>87</sup> These results confirmed the merits of ChCl–urea DES-based solvothermal doping of nitrogen into the pristine biochar for advanced oxidation application.

Moreover, loading metal oxides onto BCMs is also an efficient method for catalyzing PDS to generate free radicals. For example, Guo *et al.*<sup>45</sup> prepared a  $\text{MgFe}_2\text{O}_4$ -doped BCM from the solid fraction of wheat straw after pretreatment with a ChCl–LA DES for PDS activation. They observed that the BCM loaded with bimetallic oxides activated PDS, achieving an abidol decomposition efficiency of over 82% at pH 3–11 and explored its capability to remove other organic pollutants, such as achieving an 86.7% removal efficiency for methyl orange (Fig. 13). However, there is still a need to specify whether the pretreated solid fraction is better than the raw wheat straw for the preparation of the  $\text{MgFe}_2\text{O}_4$ -doped BCM for PDS activation.

**4.2.2 Nitrobenzene hydrogenation/reduction.** Carbon materials rich in oxygen- and nitrogen-containing groups have significant potential in the hydrogenation reduction of nitrobenzene.<sup>112–114</sup> A DES-derived BCM, abundant in carboxylic and hydroxyl groups, can thus be regarded as an effective green catalyst for the reduction of nitrobenzene. Halanur *et al.* prepared a Fe-doped DES-derived solvochar by

direct STC of  $\text{Fe}_2\text{SO}_4$ -added ChCl–EG–glucose DES.<sup>66</sup> The Fe-doped DES-derived solvochar showed a high carboxylic group content (up to  $87.8 \text{ mmol g}^{-1}$ ),<sup>66</sup> and exhibited excellent selectivity (94%) and yielded 63% of aniline, indicating superior catalytic efficiency compared to those with lower carboxylic acid content.<sup>66</sup> Similarly, in the hydrogenation reduction of nitrobenzene, Sadjadi *et al.* prepared a Pd-loaded DES-derived BCM to enhance the conversion rate and efficiency of the hydrogenation reaction.<sup>101</sup> Thus, BCMs prepared by direct STC of a glucose-containing DES and functionalized by metal catalyst doping can be developed for this application.

**4.2.3 Oxidation of alcohol.** Some carbon materials serve as stable catalyst supports, improving the dispersity and stability of metal nanoparticles, thereby enhancing catalytic activity. Notably, loaded metal catalysts, especially gold, palladium, and platinum, exhibit high activity in alcohol oxidation, making them highly effective for such processes.<sup>115–117</sup> The incorporation of nitrogen into a BCM can introduce active sites and enhance  $\pi$ -electron flow, potentially altering the electron density at the metal centers and thereby increasing their catalytic activity.<sup>118–121</sup>

Zahra Alizadeh *et al.* utilized KIT-6 as a template and prepared a DES from ChCl and glucose, with urea and guanine added to increase the nitrogen source, resulting in the production of mesoporous carbon for loading Pd nanoparticles.<sup>26</sup> The study found that this method achieved a nitrogen doping level of 9.6%, and the catalyst showed excellent performance in the catalytic oxidation of benzyl alcohol to benzoic acid, with a yield of over 99%.<sup>26</sup> Furthermore, the catalytic oxidation



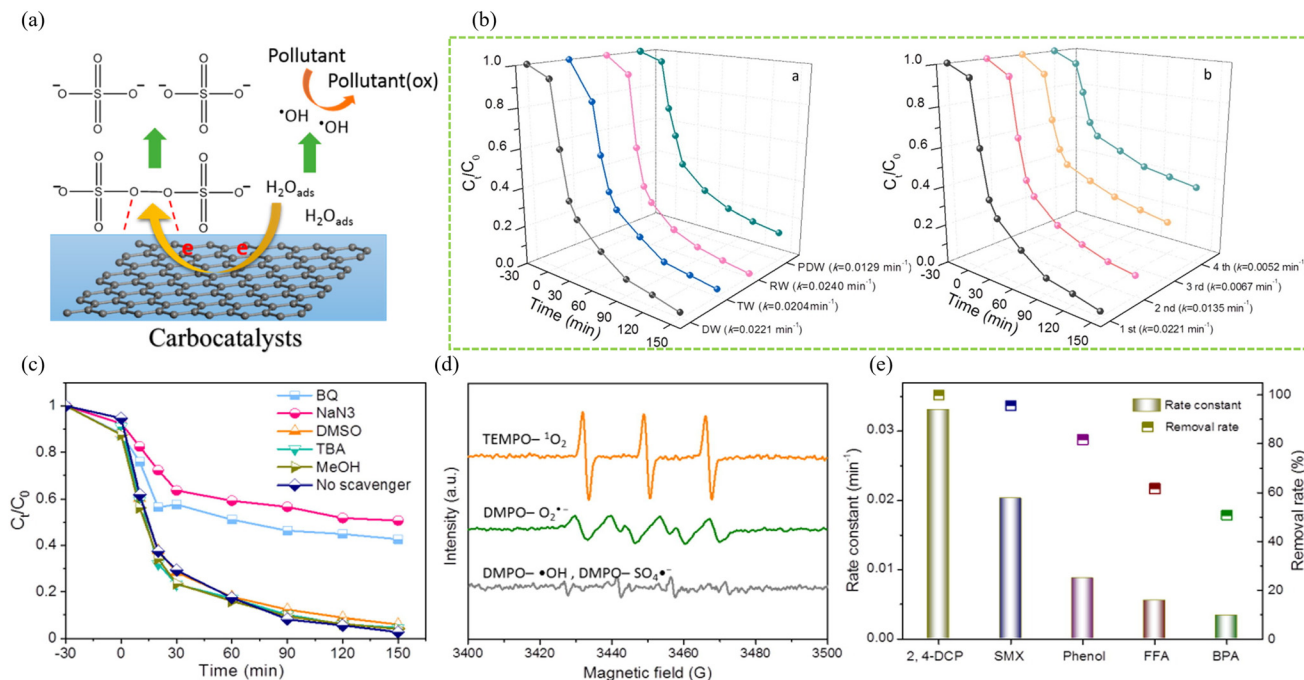


**Fig. 13** (a) Proposed mechanism of PS activation on carbocatalysts.<sup>111</sup> With permission. Copyright 2015 American Chemical Society. (b) TC removal in different water samples in the NRBF/PDS system and cycling performance of NRBF for PDS activation. (c) Quenching experiments of the carbon material under different scavengers. (d) EPR spectrum of species adducts in the NRBF/PDS system at reaction for 5 min (e) Degradation of various organics by carbon material catalyzed PDS activation.<sup>45</sup> With permission. Copyright 2021 Elsevier.

of electron-rich and electron-deficient benzyl alcohol derivatives under mild conditions and low catalyst loading demonstrated exceptional catalytic performance, delivering the corresponding carboxylic acids with excellent yields.<sup>26</sup> Moreover, the catalyst could be reused at least 10 times without a significant decrease in activity and selectivity.<sup>26</sup> This underscores the potential of nitrogen-doped mesoporous carbon materials as effective supports for metal nanoparticle catalysts in the oxidation of alcohols, offering high efficiency and recyclability.<sup>26</sup>

**4.2.4 Water splitting.** The combination of a metal and nitrogen-doped porous carbon is an effective strategy to enhance the activity and stability of catalysts. Hence, catalysts composed of transition metals (Fe, Co, and Ni) and their hybrids, as well as nitrogen-doped carbon materials, have attracted widespread attention for water splitting applications.<sup>122–127</sup> For example, Li *et al.* used a biomass-based ternary DES as both a precursor and self-template to prepare a hybrid of nitrogen-doped porous carbon loaded with cobalt nanoparticles. They reported that the derived carbon prepared at a pyrolysis temperature of 800 °C exhibited superior hydrogen evolution reaction (HER) activity. In a 0.5 M H<sub>2</sub>SO<sub>4</sub> solution, it required only 215 mV to reach a current density of 10 mA cm<sup>-2</sup>. To achieve the same current density in a 1 M KOH solution, 274 mV was needed, with a Tafel slope of 70 mV dec<sup>-1</sup>. After 1000 cycles of cyclic voltammetry, the overpotential slightly increased, indicating the catalyst's notable stability.<sup>78</sup>

### 4.3 Energy storage

**4.3.1 Electrochemical energy storage.** Carbon materials, due to their high specific surface area, good electrical conductivity, and microporous characteristics, have been proven to be excellent candidates for high-specific-capacity supercapacitors.<sup>128–130</sup> The unique properties of DESs, such as their ability to guide the formation of pores during the carbonization process and the ease of doping with heteroatoms like nitrogen through a direct carbonization process, have garnered extensive attention in the preparation of electrode materials.<sup>22,131,132</sup> For instance, Huang *et al.* utilized a DES to pretreat poplar wood powder and synthesize porous carbon electrode materials and DES gel electrolytes. After DES pretreatment and subsequent activation with NaOH, the material exhibited a higher specific surface area (1125 m<sup>2</sup> g<sup>-1</sup>) and total pore volume (0.55 cm<sup>3</sup> g<sup>-1</sup>) compared to ordinary lignin activated with NaOH and pure lignin. The fabricated supercapacitor demonstrated a maximum specific capacitance of 181.5 F g<sup>-1</sup> at a current density of 1 A g<sup>-1</sup>, surpassing the performance of hydrogel samples (140 F g<sup>-1</sup> and 113.3 F g<sup>-1</sup>). At an increased current density of 5 A g<sup>-1</sup>, the capacitance retention rate was 79.5%. Additionally, the device delivered a high energy density of 40.8 W h kg<sup>-1</sup> at a power density of 599.9 W kg<sup>-1</sup>. Notably, at an ultra-high power density of 3.2 kW kg<sup>-1</sup>, the energy density still remained at 29.0 W h kg<sup>-1</sup>.<sup>27</sup>

**4.3.2 Oxygen reduction reaction.** In traditional fuel cells, the cathode catalyst materials typically comprise platinum



(Pt) and its alloys, known for their relatively low overpotentials and high current densities during the oxygen reduction reaction (ORR).<sup>133</sup> However, the high cost and scarcity of Pt limit its widespread use and development. Research by Guo *et al.* and Yu *et al.* indicates that nitrogen doping can effectively enhance ORR activity,<sup>134,135</sup> and Chen *et al.* have demonstrated that ORR activity stems from the doping itself, rather than from metal impurities.<sup>136</sup> The abilities of DESs to directly introduce nitrogen into carbon materials during their preparation have garnered extensive attention.<sup>137</sup> For instance, Luo *et al.* used tannic acid and urea to prepare a DES, with ZnCl<sub>2</sub> as a template to produce nitrogen-rich porous graphitic carbon (Fig. 14). The study showed that the prepared material had a nitrogen atom percentage as high as 11.9%, with pyridinic nitrogen reaching 4.4%. Moreover, its half-wave potential ( $E_{1/2}$ ) was 0.84 V, very close to that of commercial Pt/C catalysts. Additionally, it outperformed Pt/C catalysts in methanol tolerance tests and durability (after running for 20 000 seconds, the current density only decreased by 6%, and there was no significant change in current density upon methanol injection).<sup>138</sup>

#### 4.4 Biological applications

**4.4.1 Biocatalysis.** So far, diverse materials have been developed for enzyme immobilization. Generally, materials with rich functional groups, like carboxylic groups and nitrogen-containing groups, are favorable for enzyme immobilization. Recent results have suggested that the BCMS prepared by STC in DESs are rich in these functional groups. Thus, they are potential carriers for enzymes. For instance, Aruchamy *et al.* employed a DES prepared from ChCl and FeCl<sub>3</sub> as both a soft template and catalyst to produce BCMS *via* STC of biomass in the DES. By loading cytochrome C (Cyt C) onto the resultant BCMS, their protein-friendly properties were explored. The results showed that the peroxidase activities of Cyt C loaded on the BCMS prepared under various conditions were either enhanced or maintained compared to those of pure Cyt C. Notably, the BCM prepared at 180 °C for 18 h demonstrated the highest efficacy, showing a 150% increase in activity.<sup>24</sup>

**4.4.2 Bio-imaging.** The CDs are emerging as a novel and promising fluorescent materials with low toxicity, widely recognized for their applications in biological imaging.<sup>139–143</sup> The incorporation of DESs in the preparation of CDs not only capi-

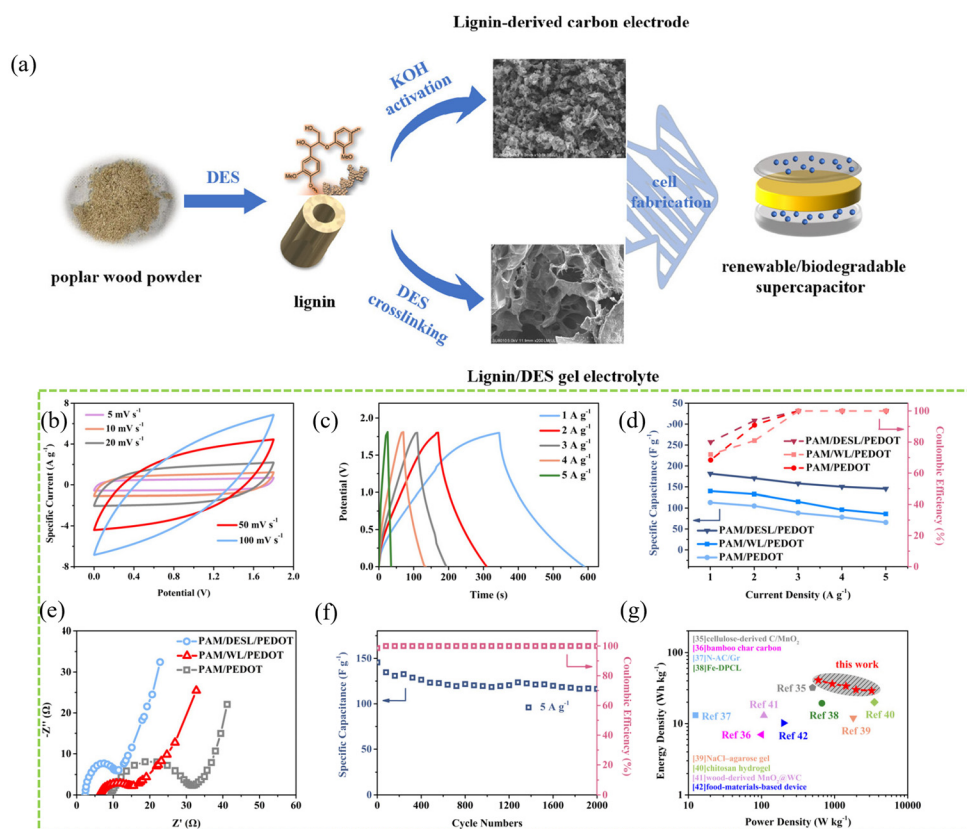


**Fig. 14** (a) The preparation process of porous carbon for high-energy supercapacitors. (b) CV curves of the PAM/DESL/PEDOT electrolyte at various scan rates. (c) GCD profiles with a current density of 1–5 A g<sup>-1</sup>. (d) Gravimetric specific capacitances and coulombic efficiencies with increasing current density in the devices. (e) Nyquist plots of the samples from EIS. (f) Cycling stability and coulombic efficiency of the PAM/DESL/PEDOT electrolyte at 5 A g<sup>-1</sup> for 2000 cycles. (g) Ragone plots of the proposed device and previously reported renewable supercapacitors.<sup>138</sup> With permission. Copyright 2022 American Chemical Society.



talizes on their green, low-toxicity, and excellent biocompatibility properties but also facilitates the doping of CDs with nitrogen and chlorine. Nitrogen-doped CDs exhibit enhanced luminescence properties, and the produced CDs possess a rich array of functional groups, offering selective probes for cellular imaging and detection.<sup>144,145</sup>

For example, Wang *et al.* developed a new method for preparing nitrogen and chlorine co-doped dual-functional CDs using a ChCl–Gly DES.<sup>145</sup> Specifically, CDs prepared *via* a DES contained abundant amino and hydroxyl groups, making them easily protonated and deprotonated. Additionally, chlorine-doped CDs are prone to forming hydrogen bonds, providing further motivation for sensitive pH detection.<sup>145</sup> This makes them highly sensitive to pH values, with a linear relationship between the fluorescence intensity of the CDs and the pH of the medium.<sup>145</sup> They exhibit good fluorescence performances even in high salt concentrations and can perform fluorescence detection of HeLa cells, under excitation at 405, 488, and 559 nm (emitting strong blue, green, and red fluorescence, respectively).<sup>145</sup> Furthermore, the fluorescence intensity in HeLa cells increased with incubation time, peaking at 5 h.<sup>145</sup>

#### 4.5 Sensing and detection

Utilizing DESs for the solvothermal synthesis of CDs presents a simple and green approach for metal detection. For example, Guo *et al.* proposed an efficient method to utilize wheat straw, treating it with a DES to extract a lignin-containing DES. This mixture was then processed in a hydrothermal autoclave at 180 °C for 6 h, followed by centrifugation, filtration, and freeze-drying to obtain lignin-derived CDs (LCDs).<sup>45</sup> The produced LCDs, with an average diameter of 1.1 nm, exhibited excellent dispersibility in aqueous solutions. The results showed that with increasing concentrations of Fe<sup>3+</sup> ions, from 10 to 1200 μM, the blue emission at 470 nm was significantly quenched, especially between 10 and 50 μM, where the quenching efficiency correlated directly with the concentration of Fe<sup>3+</sup> ions.<sup>45</sup> This phenomenon is likely due to the rich surface groups on the produced LCDs, where Fe<sup>3+</sup> ions coordinate with the –COOH/OH groups at the edge of LCDs, linking multiple LCDs together and causing photoluminescence quenching due to LCD aggregation. Moreover, LCDs could selectively recognize Fe<sup>3+</sup> ions in the presence of various interfering ions without significant fluorescence quenching by other ions.<sup>45</sup>

Additionally, Jiang *et al.* prepared nitrogen-doped hemi-cellulose carbon quantum dots (N–H–CQDs) using hemi-cellulose as the raw material and a ChCl–urea DES as both the solvent and nitrogen source.<sup>70</sup> The resultant CD, with an average particle size of 5.4 nm and rich in functional groups, exhibited the strongest photoluminescence (PL) emission at 436 nm.<sup>70</sup> With a quantum yield (QY) of 23.45% based on quinine sulfate and excellent pH and time stability, N–H–CQDs showed significant fluorescence quenching induced by Ag<sup>+</sup> ions, unlike other metal ions except Cu<sup>2+</sup>, indicating high selectivity for Ag<sup>+</sup> detection with a detection limit of 21 nM.<sup>70</sup>

Furthermore, the N–H–CQD–Ag complex could act as an “off-on” sensing probe for L-Cys detection, with a detection limit of 242 nM.<sup>70</sup> By altering the composition of the DES, the biomass raw material, and the reaction conditions, different CDs can be prepared for detecting various heavy metals. For instance, Huang *et al.* used tea residue as the biomass feedstock and varied the ratio of ChCl to urea in the DES (1 : 1, 1 : 2, and 1 : 3), as well as the preparation conditions to study the impact of these factors on CD synthesis.<sup>73</sup> The optimal conditions were achieved by using the DES composed of ChCl and urea at a molar ratio of 1 : 2 at 200 °C for 8 h.<sup>73</sup> Under these conditions, the yield and quantum yield of CDs were 2.25% and 16.99%, respectively. These CDs were applied for Cd<sup>2+</sup> detection, showing a good linear relationship from 0 μg mL<sup>-1</sup> to 20 μg mL<sup>-1</sup>, with a detection limit of 2.14 μg/mL (Fig. 15).<sup>73</sup>

## 5. Challenges and prospects

As discussed above, great progress has been achieved in the preparation and functionalization of BCMs *via* using DESs as pretreatment solvents, carbon precursors, dopants, soft templates, STC media, activation agents, and post-modification agents. Among these, the application of DESs as the media for STC is attracting more interest, owing to its various merits, such as the potential recyclability of the used DESs, and the out-performed surface structure of BCMs from DES-mediated STC. However, the application of DESs for the preparation and functionalization of BCMs is still at its fledgling state. Hence, there are several challenges to be addressed.

### 5.1 Recycling of DESs

The recyclability of DESs should be considered when they are used as pretreatment solvents, soft templates or STC media. Actually, full recovery of DESs seems impossible, attributed to the fact that part of the components will react with biomass or the BCM through esterification between hydroxyl and carboxyl groups, undergo thermochemical reactions, *e.g.*, dehydration and condensation, or even undergo decomposition. The amount of DESs used to produce the BCM *via* STC is much higher than the amount of feedstock reported in the literature. The recovery of the valuable components after STC facilitates the reduction of cost during its practical application. Thus, the recyclability of DESs and the DES recycling process should be considered when the valuable DESs are used as the media for BCM preparation.

### 5.2 Unveiling the reaction mechanisms and controlling pattern for DES-mediated STC

Although the introduction of DESs in the preparation of BCMs has yielded fascinating results, the involvement of solvents also means that they significantly influence the structure and performance of the biomass carbon during the solvothermal carbonization process. As solvothermal carbonization emerges as a novel carbonization method, there exists a lack of understanding regarding its processes and mechanisms. Specifically,



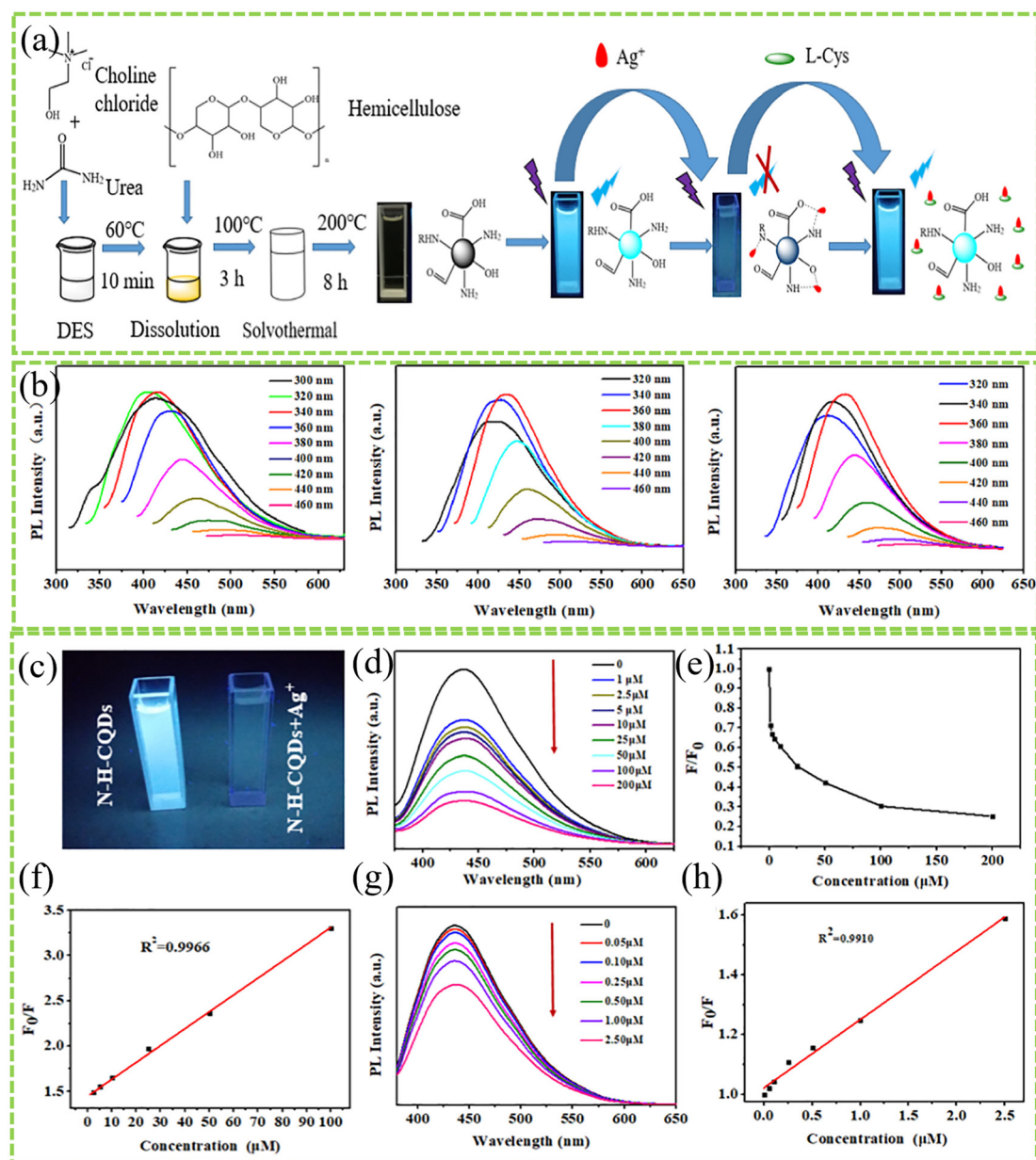


**Fig. 15** (a) Schematic of the preparation of N-H-CQDs and their detection of Ag and L-cysteine. (b) Photoluminescence emission spectra of N-H-CQDs with variations of excitation wavelength. (c) The fluorescence images of N-H-CQD solutions without (left) and with the presence of Ag ions under irradiation with UV light. (d) The PL emission spectral response of N-H-CQDs with increasing Ag concentrations (from top to bottom: 0, 1, 2.5, 5, 10, 20, 50, 100, and 200  $\mu\text{M}$ ). (e) Relative PL intensity of N-H-CQDs in the function of Ag concentrations. (f) The linear relationship between  $F^{++}_0/F$  and the concentrations of Ag ranging from 2.5  $\mu\text{M}$  to 100  $\mu\text{M}$ . (g) The fluorescence response of N-H-CQDs with increasing Ag concentrations (from top to bottom: 0, 0.05, 0.1, 0.25, 0.5, 1 and 2.5  $\mu\text{M}$ ). (h) The linear relationship between  $F^{++}_0/F$  and the concentrations of Ag ranging from 0  $\mu\text{M}$  to 2.5  $\mu\text{M}$ .<sup>73</sup> With permission. Copyright 2021 Elsevier.

the regulatory rules and formation mechanisms of biomass carbon structural characteristics under STC conditions, especially when employing DESs as novel solvents, remain unclear.

A variety of biomass sources, from raw biomass (e.g., shrimp shell,<sup>68</sup> poplar wood,<sup>88</sup> corn stalk,<sup>88</sup> cotton stalk,<sup>23</sup> garden waste,<sup>63</sup> *Parthenium hysterophorus* leaf,<sup>24</sup> and tea residue<sup>73</sup>) to biomass derivatives (e.g., glucose,<sup>66,68,75,103</sup> alginate,<sup>67</sup> hemi-

cellulose,<sup>70</sup> lignin,<sup>69</sup> and carob molasses<sup>72</sup>) have been utilized as carbon sources for the preparation of CDs or solvochar *via* the STC in DESs. For a specific application, it is more economical to utilize the low value raw biomass. Unlike the commonly used pyrolysis and HTC routes, little is known about the property differences among the BCMs from different feedstocks.

DESs can be prepared from various HBAs and HBDs. Recently, a variety of DESs were used as the STC media for the



preparation of BCMs. For example, Aruchamy *et al.* obtained tendril-like carbon helices using the DES composed of ChCl and FeCl<sub>3</sub> (1 : 2 molar ratio) as the STC media,<sup>24</sup> while Lai *et al.* obtained a BCM co-enriched with carboxyl and phenol groups by using a DES composed of ChCl and CA (1 : 1 molar ratio) as the STC medium.<sup>23</sup> Thus, BCMs with distinct properties might be obtained from STC in different DESs. More efforts are needed to elucidate the impact of DES components on the properties of resultant BCMs.

### 5.3 Developing novel applications based on the structure of BCMs from DES-mediated STC

The dominant applications of the BCMs prepared or functionalized by the involvement of DESs are focused on the environment, energy storage, and catalysis, which are too common. Since there are large amounts of existing BCMs prepared *via* various routes for these routine applications, the necessity and the progressiveness of the utilization of DESs for the preparation of functional BCMs should be specified in future studies. Techno-economic and life cycle assessments are suggested to be conducted in future studies to show the merits of the utilization of DESs for the preparation of functional BCMs.

In addition, the bio-application of BCMs, *e.g.*, bio-imaging, antioxidant, and antibacterial applications, should be enhanced. The results from Lai *et al.*<sup>23</sup> and Zhang *et al.*<sup>88</sup> showed that the BCMs prepared *via* solvothermal carbonization in DESs were highly efficient in heavy metal reduction. Thus, the resultant BCMs might be robust in donating electrons, which might facilitate their application in antioxidation and antibacterial fields. More attention should be paid to the emerging applications of BCMs, not the routine application fields.

## 6. Conclusions

DESs are promising tools in the preparation of functionalized BCMs. Utilizing DESs as precursors, doping agents, soft templates, and media that participate both directly and indirectly in the carbonization process can lead to the production of more efficient, superior-performance, eco-friendly, and sustainable materials. Moreover, promising results have been shown across various applications. This can be attributed to the unique appeal of eutectic solvent systems. Solvothermally carbonized materials prepared using DESs can introduce effective doping, such as nitrogen or iron doping, in a single step, while also enriching the materials with a variety of functional groups. However, a comprehensive understanding of the mechanisms behind the synthesis of these materials and the optimization of their properties for specific applications requires further research. Moreover, the scalability and cost-effectiveness of producing BCMs through DES modification present challenges. Despite these challenges, the potential of using DESs to prepare BCMs is immense and warrants further investigation in the future.

## Abbreviations

DES	Deep eutectic solvent
ES	Eutectic system
BCMs	Biomass-derived carbonaceous materials
STC	Solvothermal carbonization
HTC	Hydrothermal carbonization
ITC	Ionothermal carbonization
HBA	Hydrogen bond acceptor
HBD	Hydrogen bond donor
ChCl	Choline chloride
CA	Citric acid
AC	Activated carbon
LA	Lactic acid
GMA	Glycidyl methacrylate
AA	Acrylic acid
LCDs	Lignin carbon dots
CDs	Carbon dots
MBC	MgFe <sub>2</sub> O <sub>4</sub> loaded BCM
N-H-CQDs	Nitrogen-doped hemicellulose carbon quantum dots
LFA	Lignin fiber aerogel
PVA	Polymer polyvinyl alcohol
CNF	Cellulose nanofiber
(Co@NPC)	Co nanoparticle-supported nitrogen-doped porous carbon
OFGs	Oxygenated functional groups
TsOH	<i>p</i> -Toluenesulfonic acid monohydrate
ChOH	Choline hydroxide
MG	Malachite green
MB	Methylene blue
PDS	Peroxodisulfate
Hal	Halloysite
HER	Hydrogen evolution reaction
ORR	Oxygen reduction reaction
Cyt C	Cytochrome C
PL	Photoluminescence
QY	Quantum yield
ROS	Reactive oxygen species
Gly	Glycerol
EG	Ethylene glycol
ILS	Ionic liquids

## Data availability

Data availability is not applicable to this article as no new data were created or analyzed in this study.

## Author contributions

Lichun Dai: conceptualization, supervision, funding acquisition, writing – original draft, and writing – review & editing. Yiyi Shen: investigation, visualization, and writing – original draft. Haiqin Zhou: investigation, visualization, and writing –



original draft. Xiaotong He: investigation and visualization. Feng Shen: conceptualization and writing – review & editing. Zhixiang Xu: conceptualization and writing – review & editing. Bo Yang: writing – review & editing. Lingzhao Kong: writing – review & editing.

## Conflicts of interest

The authors declare that they have no known competing financial interests or personal relationships that could have appeared to influence the work reported in this paper.

## Acknowledgements

This work was supported by the Science and Technology Project of Sichuan Province (2022YFN0029), the Central Public-Interest Scientific Institution Basal Research Fund for Chinese Academy of Agricultural Sciences (1610012022013-03102), and the Science and Technology Innovation Project of Chinese Academy of Agricultural Sciences (CAAS-ASTIP-2016-BIOMA).

## References

- H. Q. Li, X. J. He, T. T. Wu, B. Y. Jin, L. Yang and J. S. Qiu, *Fuel Process. Technol.*, 2022, **230**, 18.
- Q. Sun, G. F. Zeng, J. Li, S. Wang, M. Botifoll, H. Wang, D. P. Li, F. J. Ji, J. Cheng, H. Y. Shao, Y. H. Tian, J. Arbiol, A. Cabot and L. J. Ci, *Small*, 2023, **19**, 8.
- J. Yin, W. L. Zhang, N. A. Alhebshi, N. Salah and H. N. Alshareef, *Small Methods*, 2020, **4**, 31.
- C. Zhang, W. Q. Shen, K. Guo, M. Xiong, J. Zhang and X. Lu, *J. Am. Chem. Soc.*, 2023, **145**, 10.
- Y. B. Yang, X. D. Yang, L. Liang, Y. Y. Gao, H. Y. Cheng, X. M. Li, M. C. Zou, A. Y. Cao, R. Z. Ma, Q. Yuan and X. F. Duan, *Science*, 2019, **364**, 1057–1062.
- R. Q. Ye, D. K. James and J. M. Tour, *Adv. Mater.*, 2019, **31**, 15.
- X. Gao, H. Liu, D. Wang and J. Zhang, *Chem. Soc. Rev.*, 2019, **48**, 908–936.
- F. Wu, Z. Zhou, S. Temizel-Sekeryan, R. M. Ghamkhar and A. L. Hicks, *J. Cleaner Prod.*, 2020, **270**, 11.
- J. Munuera, L. Britnell, C. Santoro, R. Cuellar-Franca and C. Casiraghi, *2D Mater.*, 2022, **9**, 45.
- L. Dai, Q. Lu, H. Zhou, F. Shen, Z. Liu, W. Zhu and H. Huang, *J. Hazard. Mater.*, 2021, **420**, 126547.
- Z. Sun, L. Dai, P. Lai, F. Shen, F. Shen and W. Zhu, *Carbon Res.*, 2022, **1**, 32.
- M. H. Mruthunjayappa, N. S. Kotrapanavar and D. Mondal, *Prog. Mater. Sci.*, 2022, **126**, 100932.
- W.-J. Liu, H. Jiang and H.-q. Yu, *Energy Environ. Sci.*, 2019, **12**, 1751–1779.
- L. Yang, C. Liang, F. Shen, M. Hu, W. Zhu and L. Dai, *J. Environ. Manage.*, 2023, **332**, 117318.
- L. Dai, W. Zhu, L. He, F. Tan, N. Zhu, Q. Zhou, M. He and G. Hu, *Bioresour. Technol.*, 2018, **267**, 510–516.
- S. Gadipelli, C. A. Howard, J. Guo, N. T. Skipper, H. Zhang, P. R. Shearing and D. J. L. Brett, *Adv. Energy Mater.*, 2020, **10**, 1903649.
- L. Dai, B. Wu, F. Tan, M. He, W. Wang, H. Qin, X. Tang, Q. Zhu, K. Pan and Q. Hu, *Bioresour. Technol.*, 2014, **161**, 327–332.
- S. A. Nicolae, H. Au, P. Modugno, H. Luo, A. E. Szego, M. Qiao, L. Li, W. Yin, H. J. Heeres, N. Berge and M. M. Titirici, *Green Chem.*, 2020, **22**, 4747–4800.
- L. Cibien, M. Parot, P. N. Fotsing, P. Gaveau, E. D. Woumfo, J. Vieillard, A. Napoli and N. Brun, *Green Chem.*, 2020, **22**, 5423–5436.
- Y. C. Liu, B. B. Huang, X. X. Lin and Z. L. Xie, *J. Mater. Chem. A*, 2017, **5**, 13009–13018.
- S. Aldroubi, M. El-Sakhawy, S. Kamel, P. Hesemann, A. Mehdi and N. Brun, *Green Chem.*, 2023, **25**, 10.
- J. Wu, Q. Liang, X. Yu, Q.-F. Lü, L. Ma, X. Qin, G. Chen and B. Li, *Adv. Funct. Mater.*, 2021, **31**, 2011102.
- P. Lai, H. Zhou, Z. Niu, L. Li, W. Zhu and L. Dai, *Chem. Eng. J.*, 2023, **457**, 141255.
- K. Aruchamy, M. Bisht, P. Venkatesu, D. Kalpana, M. R. Nidhi, N. Singh, D. Ghosh, D. Mondal and S. K. Nataraj, *Green Chem.*, 2018, **20**, 3711–3716.
- S. Long, Y. Feng, Y. Liu, L. Zheng, L. Gan, J. Liu, X. Zeng and M. Long, *Sep. Purif. Technol.*, 2021, **254**, 117577.
- S. Zahra Alizadeh, B. Karimi and H. Vali, *ChemCatChem*, 2022, **14**, e202101621.
- J. Huang, Y. Hu, H. Wang, T. Wang, H. Wu, J. Li, Y. Li, M. Wang and J. Zhang, *ACS Appl. Energy Mater.*, 2022, **5**, 6393–6400.
- A. Sultana, R. W. Cheatham and M. T. Reza, *J. CO2 Util.*, 2023, **68**, 10.
- C. Padwal, H. D. Pham, L. T. M. Hoang, S. Mundree and D. Dubal, *Sustainable Mater. Technol.*, 2023, **35**, 10.
- F. Hussin, M. K. Aroua and R. Yusoff, *J. Environ. Chem. Eng.*, 2021, **9**, 105333.
- T. Ariyanto, K. Masruroh, G. Y. S. Pambayun, N. I. F. Mukti, R. B. Cahyono, A. Prasetya and I. Prasetyo, *ACS Omega*, 2021, **6**, 19194–19201.
- A. F. Arangadi, J. K. Ali, M. Abi Jaoude, D. H. Anjum, A. Alkhoori, K. Polychronopoulou and E. Alhseinat, *Desalination*, 2022, **530**, 12.
- B. B. Hansen, S. Spittle, B. Chen, D. Poe, Y. Zhang, J. M. Klein, A. Horton, L. Adhikari, T. Zelovich, B. W. Doherty, B. Gurkan, E. J. Maginn, A. Ragauskas, M. Dadmun, T. A. Zawodzinski, G. A. Baker, M. E. Tuckerman, R. F. Savinell and J. R. Sangoro, *Chem. Rev.*, 2021, **121**, 1232–1285.
- D. K. Yu, Z. M. Xue and T. C. Mu, *Chem. Soc. Rev.*, 2021, **50**, 8596–8638.
- D. K. Yu, Z. M. Xue and T. C. Mu, *Cell Rep. Phys. Sci.*, 2022, **3**, 23.
- G. Sima, L. Gan, L. Chang, Y. Cui and R. K. Kankala, *Microporous Mesoporous Mater.*, 2021, **323**, 111192.



- 37 Y. Y. Chia and L. W. Yoon, *J. Environ. Sci.*, 2018, **13**, 52–66.
- 38 A. Jain, S. Jayaraman, R. Balasubramanian and M. P. Srinivasan, *J. Mater. Chem. A*, 2014, **2**, 520–528.
- 39 G. Sun, L. Qiu, M. Zhu, K. Kang and X. Guo, *Ind. Crops Prod.*, 2018, **125**, 41–49.
- 40 P. Nantnarphirom, W. Kraithong, N. Viriya-empikul and A. Eiad-ua, *Organosolv pretreatment transformation process of bagasse to porous carbon material*, Pattaya, Thailand, 2016.
- 41 Y. Wang, H. Wang, L. Chen, W. T. Wang, Z. H. Yang, Z. M. Xue and T. C. Mu, *Green Chem.*, 2023, **25**, 4685–4695.
- 42 H. T. Yu, Z. M. Xue, R. F. Shi, F. Y. Zhou and T. C. Mu, *Ind. Crops Prod.*, 2022, **184**, 9.
- 43 Q. L. Liu, X. H. Zhao, D. K. Yu, H. T. Yu, Y. B. Zhang, Z. M. Xue and T. C. Mu, *Green Chem.*, 2019, **21**, 5291–5297.
- 44 H. X. Han, L. Chen, J. C. Zhao, H. T. Yu, Y. Wang, H. L. Yan, Y. X. Wang, Z. M. Xue and T. C. Mu, *Acta Phys.-Chim. Sin.*, 2023, **39**, 11.
- 45 J. Guo, J. Xu, X. Liu, L. Dai, C. Zhang, X. Xiao and K. Huo, *J. Hazard. Mater.*, 2022, **435**, 129072–129072.
- 46 Z.-X. Xu, X.-Q. Ma, Y.-Q. Shan, B. Li, S. M. Osman, P.-G. Duan and R. Luque, *Chemosphere*, 2022, **308**, 135840.
- 47 M. T. Islam, A. I. Sultana, N. Saha, J. L. Klinger and M. T. Reza, *Ind. Eng. Chem. Res.*, 2021, **60**, 15479–15491.
- 48 Z. Ma, J. Wang, Y. Deng, Y. Wang and L. Yan, *Biomacromolecules*, 2021, **22**, 4181–4190.
- 49 C. Alvarez-Vasco, R. Ma, M. Quintero, M. Guo, S. Geleyense, K. K. Ramasamy, M. Wolcott and X. Zhang, *Green Chem.*, 2016, **18**, 5133–5141.
- 50 Z. Chen, X. Bai, A. Lusi and C. Wan, *ACS Sustainable Chem. Eng.*, 2018, **6**, 12205–12216.
- 51 F. del Monte, D. Carriazo, M. C. Serrano, M. C. Gutiérrez and M. L. Ferrer, *ChemSusChem*, 2014, **7**, 999–1009.
- 52 G. Carrasco-Huertas, R. J. Jiménez-Riobóo, M. C. Gutiérrez, M. L. Ferrer and F. del Monte, *Chem. Commun.*, 2020, **56**, 3592–3604.
- 53 Y. M. Cui, M. He, R. Dai, H. Chen and Y. Q. Wang, *J. Am. Leather Chem. Assoc.*, 2023, **118**, 95–101.
- 54 S. N. Wang, L. L. Zhang, R. T. Ma, J. Yu, X. Y. Zhang, C. Shi, L. S. Ma, T. Q. Li, Y. F. Huang, Y. L. Hu, Y. M. Fan and Z. G. Wang, *Chem. Eng. J.*, 2023, **454**, 12.
- 55 M. Wang, Z. B. Lai, X. L. Jin, T. L. Sun, H. C. Liu and H. S. Qi, *Adv. Funct. Mater.*, 2021, **31**, 2101957.
- 56 Y. Ahn, S. H. Lee, H. J. Kim, Y.-H. Yang, J. H. Hong, Y.-H. Kim and H. Kim, *Carbohydr. Polym.*, 2012, **88**, 395–398.
- 57 B. Azimi, H. Maleki, V. Gigante, R. Bagherzadeh, A. Mezzetta, M. Milazzo, L. Guazzelli, P. Cinelli, A. Lazzeri and S. Danti, *Cellulose*, 2022, **29**, 3079–3129.
- 58 J. L. Shamshina and R. D. Rogers, in *Green Electrospinning*, 2019, pp. 189–216, DOI: [10.1515/9783110581393-008](https://doi.org/10.1515/9783110581393-008).
- 59 K. Rong, J. Wei, Y. Wang, J. Liu, Z. Qiao, Y. Fang and S. Dong, *Green Chem.*, 2021, **23**, 6065–6075.
- 60 X. X. Tan, W. C. Zhao and T. C. Mu, *Green Chem.*, 2018, **20**, 3625–3633.
- 61 X. X. Tan, Y. Q. Wang, W. H. Du and T. C. Mu, *ChemSusChem*, 2020, **13**, 321–327.
- 62 Z. Xu, X. Ma, J. Liao, S. M. Osman, S. Wu and R. Luque, *ACS Sustainable Chem. Eng.*, 2022, **10**, 4258–4268.
- 63 Y. Liu, Y. Cao and Q. Yu, *Biomass Bioenergy*, 2022, **167**, 106626.
- 64 Y. T. Yang, X. X. Yang, Y. T. Wang, J. Luo, F. Zhang, W. J. Yang and J. H. Chen, *Fuel*, 2018, **219**, 166–175.
- 65 X. X. Lin, B. Tan, L. Peng, Z. F. Wu and Z. L. Xie, *J. Mater. Chem. A*, 2016, **4**, 4497–4505.
- 66 M. M. Halanur, S. Chakraborty, K. Aruchamy, D. Ghosh, N. Singh, K. Prasad, D. Kalpana, S. K. Nataraj and D. Mondal, *J. Mater. Chem. A*, 2019, **7**, 4988–4997.
- 67 N. Yadav, M. M. Halanur, M. Bisht, S. K. Nataraj, P. Venkatesu and D. Mondal, *Chem. Commun.*, 2020, **56**, 9659–9662.
- 68 M. Feng, J. Yan, B. He, X. Chen and J. Sun, *Int. J. Biol. Macromol.*, 2021, **193**, 347–357.
- 69 J. K. Xu, C. T. Zhang, X. Xiao, J. Guo, X. Y. Liu, L. Dai and K. F. Huo, *J. Hazard. Mater.*, 2022, **435**, 12.
- 70 X. Jiang, J. Huang, T. Chen, Q. Zhao, F. Xu and X. Zhang, *Int. J. Biol. Macromol.*, 2020, **153**, 412–420.
- 71 H. M. Manohara, K. Aruchamy, S. Chakraborty, N. Radha, M. R. Nidhi, D. Ghosh, S. K. Nataraj and D. Mondal, *ACS Sustainable Chem. Eng.*, 2019, **7**, 10143–10153.
- 72 S. D. Calhan, M. O. Alas, M. Asik, F. N. D. Kaya and R. Genc, *J. Mater. Sci.*, 2018, **53**, 15362–15375.
- 73 Z.-Y. Huang, W.-Z. Wu, Z.-X. Li, Y. Wu, C.-B. Wu, J. Gao, J. Guo, Y. Chen, Y. Hu and C. Huang, *Ind. Crops Prod.*, 2022, **184**, 115085.
- 74 S. V. Kamath, H. M. Manohara, K. Aruchamy, A. S. Maraddi, G. B. D'Souza, K. N. Santhosh, K. N. Mahadevapradas and S. K. Nataraj, *RSC Adv.*, 2022, **12**, 9101–9111.
- 75 R. Tabaraki and F. Nazari, *Spectrochim. Acta, Part A*, 2023, **300**, 122829.
- 76 D. Mondal, M. Sharma, C.-H. Wang, Y.-C. Lin, H.-C. Huang, A. Saha, S. K. Nataraj and K. Prasad, *Green Chem.*, 2016, **18**, 2819–2826.
- 77 L. Chen, J. Deng, Y. Song, S. Hong and H. Lian, *Mater. Res. Bull.*, 2020, **123**, 110708.
- 78 D. Li, Y. Huang, Z. Li, L. Zhong, C. Liu and X. Peng, *Chem. Eng. J.*, 2022, **430**, 132783.
- 79 Z. J. Ke, M. Mei, J. X. Liu, P. Y. Du, B. Zhang, T. Wang, S. Chen and J. P. Li, *J. Cleaner Prod.*, 2022, **357**, 11.
- 80 H. Y. Mou, J. F. Wang, D. L. Zhang, D. K. Yu, W. J. Chen, D. B. Wang and T. C. Mu, *J. Mater. Chem. A*, 2019, **7**, 5719–5725.
- 81 Y. B. Zhang, Z. M. Xue, X. H. Zhao, B. L. Zhang and T. C. Mu, *Green Chem.*, 2022, **24**, 1721–1731.
- 82 A. Mukherjee, J. A. Okolie, C. Niu and A. K. Dalai, *Energy Convers. Manage.: X*, 2022, **14**, 100218.
- 83 A. Mukherjee, B. Saha, C. Niu and A. K. Dalai, *J. Environ. Chem. Eng.*, 2022, **10**, 108815.



- 84 G. Kaur, N. Singh and A. Rajor, *ChemistrySelect*, 2021, **6**, 3139–3150.
- 85 I. A. Lawal, M. Klink and P. Ndungu, *Environ. Res.*, 2019, **179**, 11.
- 86 J. Huang, S. R. Cao, Z. H. Liu, J. Tian, C. X. Xi and Z. Q. Chen, *J. Environ. Chem. Eng.*, 2022, **10**, 12.
- 87 S. Ye, W. Xiong, J. Liang, H. Yang, H. Wu, C. Zhou, L. Du, J. Guo, W. Wang, L. Xiang, G. Zeng and X. Tan, *J. Colloid Interface Sci.*, 2021, **601**, 544–555.
- 88 Y. L. Zhang, Y. H. Meng, L. Ma, H. R. Ji, X. Q. Lu, Z. Q. Pang and C. H. Dong, *J. Cleaner Prod.*, 2021, **324**, 9.
- 89 M. Kurian and A. Paul, *Carbon Trends*, 2021, **3**, 100032.
- 90 T. C. Wareing, P. Gentile and A. N. Phan, *ACS Nano*, 2021, **15**, 15471–15501.
- 91 Y. Li, Z. Tang, Z. Pan, R. Wang, X. Wang, P. Zhao, M. Liu, Y. Zhu, C. Liu, W. Wang, Q. Liang, J. Gao, Y. Yu, Z. Li, B. Lei and J. Sun, *ACS Nano*, 2022, **16**, 4357–4370.
- 92 M. C. Rong, Y. F. Feng, Y. R. Wang and X. Chen, *Sens. Actuators, B*, 2017, **245**, 868–874.
- 93 M. E. Mahmoud, N. A. Fekry and A. M. Abdelfattah, *J. Hazard. Mater.*, 2020, **397**, 122770.
- 94 Y. Xu, S. C. Sun, C. Zhang, C. Y. Ma, J. L. Wen and T. Q. Yuan, *Chem. Eng. J.*, 2023, **462**, 10.
- 95 J. H. Lee and S. J. Park, *Carbon*, 2020, **163**, 1–18.
- 96 M. L. Wang, Z. H. Zhou, J. L. Zhu, H. Lin, K. Dai, H. D. Huang and Z. M. Li, *Carbon*, 2022, **198**, 142–150.
- 97 R. Yadav, K. Aruchamy, D. Mondal and P. Venkatesu, *Colloids Surf., B*, 2020, **187**, 7.
- 98 M. Mohan, O. Demerdash, B. A. Simmons, J. C. Smith, M. K. K. Kidder and S. Singh, *Green Chem.*, 2023, **25**, 3475–3492.
- 99 H. Xiao, J. Dai, J. Kuang, J. Fan, J. Du and H. Peng, *Sep. Purif. Technol.*, 2023, **304**, 122345.
- 100 R. Zhou, C. Xu, J. Yang, D. Guan and J. Cai, *Chem. Lett.*, 2020, **49**, 585–588.
- 101 S. Sadjadi, M. Akbari, F. G. Kahangi and M. M. Heravi, *Appl. Clay Sci.*, 2020, **192**, 105640.
- 102 A. A. Pam, Z. A. M. Hir, A. H. Abdullah and Y. P. Tan, *Appl. Water Sci.*, 2021, **11**, 90.
- 103 C. Xiong, F. Liu, J. Gao and X. Jiang, *RSC Adv.*, 2020, **10**, 34953–34958.
- 104 M. S. Alam, D. Gorman-Lewis, N. Chen, S. Safari, K. Baek, K. O. Konhauser and D. S. Alessi, *Environ. Sci. Technol.*, 2018, **52**, 13057–13067.
- 105 I. A. Lawal, M. Klink and P. Ndungu, *Environ. Res.*, 2019, **179**, 11.
- 106 X. Quan, Z. Fu, L. Yuan, M. Zhong, R. Mi, X. Yang, Y. Yi and C. Wang, *RSC Adv.*, 2017, **7**, 35875–35882.
- 107 X. Gao, A. Omosebi, J. Landon and K. Liu, *Environ. Sci. Technol.*, 2015, **49**, 10920–10926.
- 108 A. F. Arangadi, J. K. Ali, M. A. Jaoude, D. H. Anjum, A. AlKhoori, K. Polychronopoulou and E. Alhseinat, *Desalination*, 2022, **530**, 12.
- 109 N. Liu, L. Zhang, Y. Xue, J. Lv, Q. Yu and X. Yuan, *Sep. Purif. Technol.*, 2017, **184**, 213–219.
- 110 H. Lee, H.-i. Kim, S. Weon, W. Choi, Y. S. Hwang, J. Seo, C. Lee and J.-H. Kim, *Environ. Sci. Technol.*, 2016, **50**, 10134–10142.
- 111 X. Duan, H. Sun, J. Kang, Y. Wang, S. Indrawirawan and S. Wang, *ACS Catal.*, 2015, **5**, 4629–4636.
- 112 W. Xiong, Z. Wang, S. He, F. Hao, Y. Yang, Y. Lv, W. Zhang, P. Liu and H. a. Luo, *Appl. Catal., B*, 2019, **260**, 118105.
- 113 X. Zhao, A. Li, X. Quan, S. Chen, H. Yu and S. Zhang, *Chemosphere*, 2019, **238**, 124636.
- 114 L. Pei, H. Tan, M. Liu, R. Wang, X. Gu, X. Ke, J. Jia and Z. Zheng, *Green Chem.*, 2021, **23**, 3612–3622.
- 115 M. Li, S. J. Wu, X. Y. Yang, J. Hu, L. Peng, L. Bai, Q. S. Huo and J. Q. Guan, *Appl. Catal., A*, 2017, **543**, 61–66.
- 116 R. Arrigo, M. E. Schuster, Z. Xie, Y. Yi, G. Wowsnick, L. L. Sun, K. E. Hermann, M. Friedrich, P. Kast, M. Haevecker, A. Knop-Gericke and R. Schloegl, *ACS Catal.*, 2015, **5**, 2740–2753.
- 117 R. Arrigo, S. Wrabetz, M. E. Schuster, D. Wang, A. Villa, D. Rosenthal, F. Girsgdies, G. Weinberg, L. Prati, R. Schlögl and D. S. Su, *Phys. Chem. Chem. Phys.*, 2012, **14**, 10523–10532.
- 118 S. S. Shang and S. Gao, *ChemCatChem*, 2019, **11**, 3728–3742.
- 119 W. Xia, *Catal. Sci. Technol.*, 2016, **6**, 630–644.
- 120 O. Y. Podyacheva and Z. R. Ismagilov, *Catal. Today*, 2015, **249**, 12–22.
- 121 V. Z. Olga, P. Olga Yu, N. S. Arina, S. K. Lidiya and A. K. Oxana, *Appl. Catal., A*, 2021, **629**, 118424.
- 122 W. Izabela, K.-K. Karolina and R. Piotr, *Int. J. Hydrogen Energy*, 2023, **48**, 25741–25754.
- 123 S. B. Devi and R. Navamathavan, *J. Electrochem. Soc.*, 2023, **170**, 026504.
- 124 Y. Chunxia, Y. Yaqi, W. Jie, H. Jianhua and S. Ziqiang, *BioChar*, 2023, **5**, 90.
- 125 C. Xia, S. Surendran, S. Ji, D. Kim, Y. Chae, J. Kim, M. Je, M. K. Han, W. S. Choe, C. H. Choi, H. Choi, J. K. Kim and U. Sim, *Carbon Energy*, 2022, **4**, 491–505.
- 126 K. Kordek, H. Yin, P. Rutkowski and H. Zhao, *Int. J. Hydrogen Energy*, 2018, **44**, 23–33.
- 127 J. Y. Jiang, C. Y. Yan, X. H. Zhao, H. X. Luo, Z. M. Xue and T. C. Mu, *Green Chem.*, 2017, **19**, 3023–3031.
- 128 H. Shao, Y.-C. Wu, Z. Lin, P.-L. Taberna and P. Simon, *Chem. Soc. Rev.*, 2020, **49**, 3005–3039.
- 129 Y. Luo, Y. Yan, S. Zheng, H. Xue and H. Pang, *J. Mater. Chem. A*, 2018, **7**, 901–924.
- 130 J. Ni and Y. Li, *Adv. Energy Mater.*, 2016, **6**, 1600278.
- 131 C.-W. Lien, B. Vedhanarayanan, J.-H. Chen, J.-Y. Lin, H.-H. Tsai, L.-D. Shao and T.-W. Lin, *Chem. Eng. J.*, 2021, **405**, 126706.
- 132 M. Zhong, Q. F. Tang, Y. W. Zhu, X. Y. Chen and Z. J. Zhang, *J. Power Sources*, 2020, **452**, 227847.
- 133 S. Sun, F. Jaouen and J.-P. Dodelet, *Adv. Mater.*, 2008, **20**, 3900–3904.
- 134 D. S. Yu, Q. Zhang and L. M. Dai, *J. Am. Chem. Soc.*, 2010, **132**, 15127–15129.



- 135 D. Guo, R. Shibuya, C. Akiba, S. Saji, T. Kondo and J. Nakamura, *Science*, 2016, **351**, 361–365.
- 136 S. Chen, J. Bi, Y. Zhao, L. Yang, C. Zhang, Y. Ma, Q. Wu, X. Wang and Z. Hu, *Adv. Mater.*, 2012, **24**, 5593–5597.
- 137 D. Carriazo, M. Concepcion Serrano, M. Concepcion Gutierrez, M. Luisa Ferrer and F. del Monte, *Chem. Soc. Rev.*, 2012, **41**, 4996–5014.
- 138 R. Luo, C. Liu, J. Li, C. Wang, X. Sun, J. Shen, W. Han and L. Wang, *ACS Appl. Mater. Interfaces*, 2017, **9**, 32737–32744.
- 139 M. E. Khan, A. Mohammad and T. Yoon, *Chemosphere*, 2022, **302**, 134815.
- 140 L.-p. Li, X.-f. Ren, P.-r. Bai, Y. Liu, W.-y. Xu, J. Xie and R.-p. Zhang, *New Carbon Mater.*, 2021, **36**, 632–638.
- 141 J. Zhong, X. Chen, M. Zhang, C. Xiao, L. Cai, W. A. Khan, K. Yu, J. Cui and L. He, *Chin. Chem. Lett.*, 2020, **31**, 769–773.
- 142 W. Yang, H. Zhang, J. Lai, X. Peng, Y. Hu, W. Gu and L. Ye, *Carbon*, 2018, **128**, 78–85.
- 143 L. Fang, S. Yuxiang, H. Hui, L. Yang, F. Yijun, H. Jian, L. Hao, Q. Huihua and K. Zhenhui, *Carbon*, 2017, **120**, 95–102.
- 144 M. Wang, X. Kang, L. Deng, M. Wang, Z. Xia and D. Gao, *Food Chem.*, 2020, **345**, 128817.
- 145 N. Wang, A.-Q. Zheng, X. Liu, J.-J. Chen, T. Yang, M.-L. Chen and J.-H. Wang, *ACS Appl. Mater. Interfaces*, 2018, **10**, 7901–7909.

